5 BATCH MLSS SETTLING EVALUATION

Traditional batch MLSS settling tests are evaluated in this chapter. The settling results illustrate the effects of temperature variations on aspects of manual MLSS settling tests in an operational plant environment.

5.1 Background

The MLSS settling and clarification processes are not evaluated continuously in an operational secondary settling tank (Gernaey *et al*., 1998). These processes are therefore simulated on laboratory scale in a test cylinder, as represented by the qualitative graphical description in Figure 5-1 (adapted from Kazami and Furumai, 2000).

A MLSS sample from a reactor is placed in a transparent test cylinder to start a batch settling test. The settling MLSS / liquid interface level is recorded for the duration of the settling interval. This settling interval consists of four settling stages: (1) reflocculation or lag, (2) zone settling, (3) transition, and (4) compression (or processes A, C, D, E). The clarification stage (process B) progresses simultaneously on top of the interface.

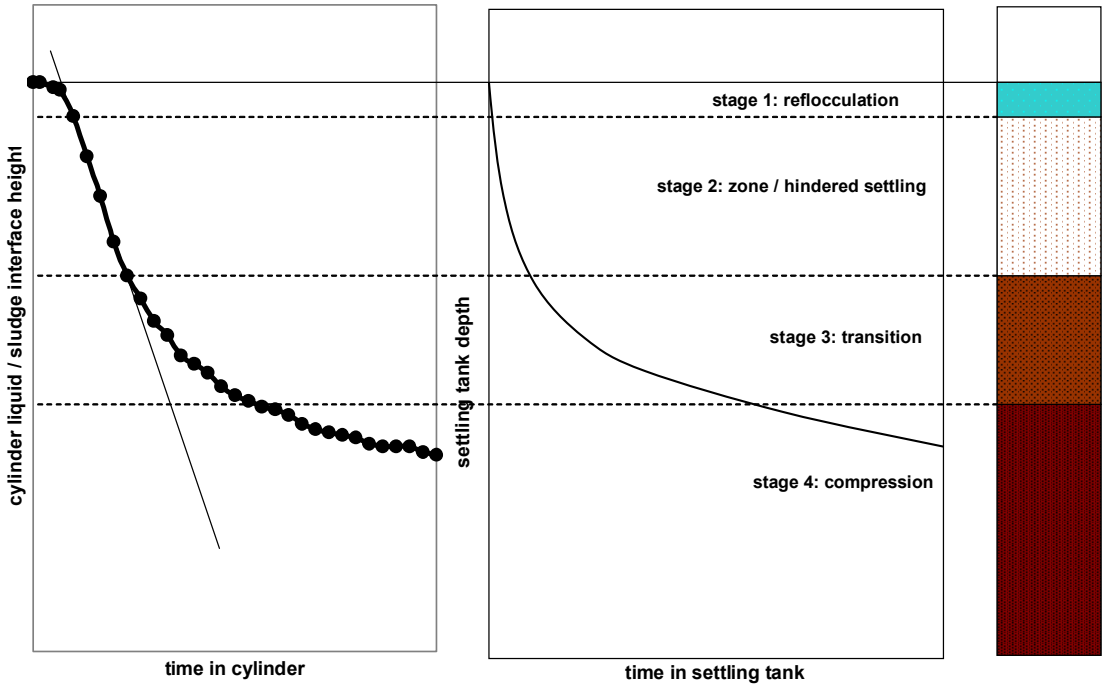

Figure 5-1 MLSS settling profiles in a cylinder and a secondary settling tank

MLSS settling tests are usually performed in a laboratory that is not located near the plant reactor. Therefore, there are time delays between the collection of MLSS samples from the reactor until the start of batch MLSS settling tests. The T_s adjusts during sample collection, transfer, storage, and settling towards the prevailing T_a.

The MLSS settling test procedures (APHA, 1998) are summarised in Table 5-1. The cylinder size, sample stirring provision, and temperature control are the most important experimental conditions that require special equipment. The recommended equipment for SV_{30} and SVI tests are stirred 1 ℓ cylinders that are temperature controlled at T_r. The ZSV test requires larger stirred columns, which must also be temperature controlled at T_r.

Table 5-1 Batch MLSS settling tests procedures (APHA, 1998)

Parameter & method	**Container**	**Temperature control**	**Stirring**	**MLSS concentration**
SV_{30}, 2710C	1ℓ transparent cylinder	Yes, at T_r	Yes, < 4 rpm	Not required
SVI, 2710D	1ℓ transparent cylinder	Yes, at T_r	Yes, < 4 rpm	standard method 2540D
ZSV, 2710E	>1 m high column >10 cm diameter	Yes, at T_r or a evaluation temperature	Yes	Not required

Parker *et al*. (2000) recommend that the purposes of batch MLSS settling tests are identified before experimental methods are finalised. If the test purpose is only preliminary diagnostic work, several relationships are available between ZSV as a function of MLSS concentration and SVI. For more reliable research work to determine ZSV, the standard methods (APHA, 1998) prescribe a settling test using a long column with temperature control facilities. Unstirred MLSS settling tests in graduated cylinders are considered as an approximation to determine SV_{30}, SVI, and ZSV. If these test purposes and methods are not considered, MLSS settling tests can lead to the misuse of settling parameters for unsuitable purposes (Dick and Vesilind, 1969), especially when large temperature effects are present.

The aim of this chapter is to use basic batch MLSS settling tests to illustrate how variations in settling parameters obtained from unstirred MLSS settling tests are related to the following aspects:

- settling parameter change in different size test cylinders,
- settling parameter change throughout the three zones of a BNR reactor, and
- settling parameter change during temperature variations.

5.2 Materials and methods

5.2.1 Experimental approach

The extent of calculated MLSS settleability changes as reported in Chapter 3, over observed operational temperature ranges as reported in Chapter 4, needs to be experimentally verified. Batch MLSS settling tests are used to determine the impact of three operational test conditions on MLSS settling parameters.

The three test conditions investigated are (i) container size, (ii) BNR reactor zone sample source, and (iii) sample environmental conditions. The settling parameters representing MLSS settleability are SVI, ISV, and supernatant turbidity.

Preliminary tests verify the suitability of a MLSS concentration meter used during temperature variations, the effect of a 1 and 2 ℓ cylinder and the MLSS sample location in a BNR reactor on settling parameters, as well as the impact of extended sample heating and cooling on MLSS settleability.

5.2.2 Settling measurement equipment

Transfer pipettes are used to draw supernatant samples from the cylinders for turbidity measurements. Turbidity is determined with a spectrophotometer (Merck Spetroquant Nova 60; Merck, 2007) calibrated in FNU (Formazine Nephelometric Unit). A hand-held MLSS concentration meter (Royce Model 711) is used for additional MLSS concentration measurements in reactor zones and batch MLSS samples. The T_s of MLSS samples are measured with a hand-held digital thermometer (Testo 925; Testo, 2007), equipped with a 60 cm immersion probe to detect the temperature in the middle of the cylinder.

5.2.3 Settling profile determination

Batch MLSS settling tests are performed in unstirred 2 ℓ graduated cylinders. The four stages of MLSS settling during the 30-minute test, which are (1) reflocculation, (2) zone settling, (3) transition, and (4) compression, are indicated in Figure 5-2 according to profile slope changes (adapted from Ekama *et al.*, 1997). At the start of MLSS settling process, the reflocculation during stage 1 leads after a lag period to the formation of a MLSS / liquid interface that begins to descend, and a changing settling profile slope is formed. Once this settling interface reaches maximum settling velocity, the linear portion of the profile indicates maximum or zone settling velocity in stage 2. A reduction in settling velocity leads to another change in the profile slope, to indicate transition in stage 3. Compression in stage 4 starts with a more stable slope that continues until the settling test duration is completed, or the MLSS / liquid interface is stationary.

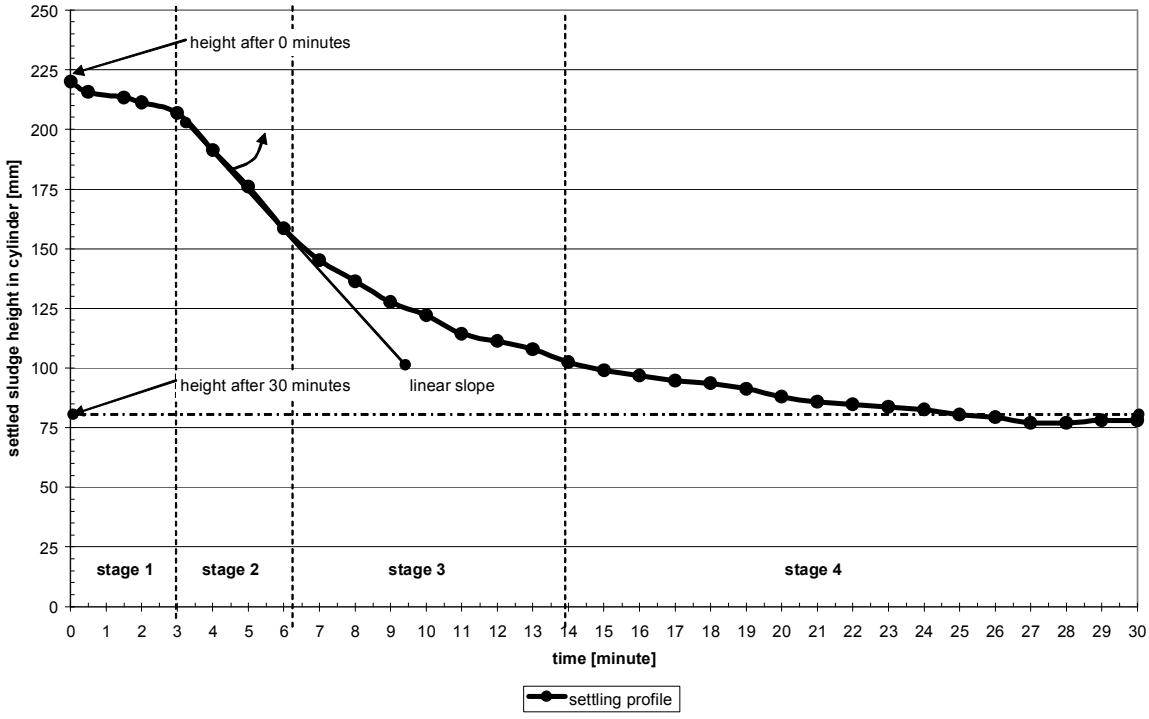

Figure 5-2 Batch MLSS settling profile with 4 settling stages

The ZSV (or u_max) is calculated from the maximum linear slope, and the time to reach ZSV (or t_umax) is determined from the start of the linear slope, as indicated in Figure 5-2. SV_{30} is obtained from the interface height or volume of settled MLSS after 30 minutes, after which SVI is calculated from this SV_{30} and the measured initial MLSS concentration.

5.2.4 Temperature impact on MLSS concentration meter reading

MLSS concentration meter measurements are based on the principle of light scattering caused by the presence of bioflocs (Vanrolleghem *et al.*, 2006). It is not known to what extend commercial MLSS concentration meter readings vary due to changes in temperature-dependent physical biofloc characteristics. MLSS samples in 2 ℓ containers are therefore heated or cooled, and restirred to measure T_s and MLSS concentrations. The measured MLSS concentrations are plotted against T_s. The Microsoft Excel curve fitting function is used to identify trends to indicate if MLSS meter readings are significantly altered by T_s variations, which may exclude the use of such meters in this study.

The MLSS concentration instrument readings decrease slightly with a T_s increase, as summarised in Table 11-2 in Appendix C. The average decrease of 14 mgSS/ℓ per 1°C T_s increase is negligible. The MLSS concentration meter is considered suitable for experimental use within the operational temperature variation range of a few degrees Celsius, as the meter reading change is less than 140 mgSS/ℓ per 10°C T_s change.

5.2.5 Settling container size

MLSS settling results in different sized containers (1 ℓ, 2 ℓ graduated cylinders, and 20 ℓ drum) are compared to determine if settling variations are evident over the MLSS concentration range. Dimensions of the graduated cylinders and the plastic drum are listed in Table 5-2. For a well-settling MLSS, even a 1 ℓ cylinder with a narrow diameter (about 60 mm) should not cause cylinder wall effects (Bhargava and Rajagopal, 1993).

Table 5-2 Batch MLSS settling tests container size

Container	Length / Width [mm]	Diameter [mm]	Height [mm]
1 ℓ	N/A	60.0	355
2 ℓ	N/A	76.8	432
20 ℓ	210 / 250	N/A	405

5.2.6 Reactor zone samples

Thirty-five sets of 2 ℓ grab MLSS samples are periodically taken from the anaerobic zone, anoxic zone, and four successive aerobic zone sections (numbered 1 and 2 from

start, 3 and 4 from end of zone) of a pilot plant BNR reactor consisting of cascading 200 ℓ drums. The piping configuration (bottom inlet, top outlet) and continuous mixing ensure zone samples are representative. MLSS concentration, DO concentration, as well as T_r are measured in all the zones. Batch MLSS settling tests are performed and settling profiles are tabulated. Clarified supernatant samples are collected to measure the turbidity. SV_{30} are obtained from the settling profiles to calculate SVI. ISV are then calculated from the settled MLSS height differences over the settling period of 2 to 5 minutes.

The reactor zone conditions in Table 11-3 in Appendix D indicate relatively stable process conditions. The DO concentrations of the anaerobic and anoxic zones are low (below 0.1 mg/ℓ), while the DO concentrations are above 2.0 mg/ℓ in most sections of the aerobic zone. The MLSS concentration is an average of about 3500 mg/ℓ, with a standard variation of less than 300 mg/ℓ. The MLSS sample settling tests are usually performed at similar conditions (middle of day), which is reflected in low standard deviations in reactor zone temperatures. The higher temperature of about 1°C in the aerobic zone 1 is due to the temporary installation of a heater probe in an attempt to control the T_r of the reactor.

5.2.7 Additional preliminary tests: extended heating and cooling

Preliminary extended heating and cooling test results are summarised in Table 11-4 in Appendix D. The results indicate that MLSS settling changes due to temperature variations are not linear. Larger settleability changes are evident at lower temperatures.

Several studies (Çetin and Sürücü, 1990; Krishna and Van Loosdrecht, 1999; Morgan-Sagastume and Allen, 2003; Zhang *et al.*, 2006b) reported poorer MLSS settling at elevated temperatures. SVI values increased (up to 540 mℓ/g) at long-term elevated temperatures as high as 35 to 45°C. These extreme temperature conditions resulted in deflocculation and reduced MLSS settling properties, as confirmed experimentally by Wilén *et al.* (2006) at 30 to 45°C, as well as at 4°C. Some of these MLSS settling studies were performed at industrial wastewater plants, as well as during long-term temperature variations. These observations illustrate the importance of proper reference conditions during MLSS settling evaluations. Empirical settling models are not valid outside the experimental temperature boundaries. This preliminary test confirmed that MLSS settleability is not directly related to temperature variations outside these experimental boundaries.

5.2.8 Sample conditioning methods

To change environmental conditions, 1 ℓ and 2 ℓ cylinders are placed in direct sunlight or in shade. The rest of the experimental method is identical to previous procedures.

5.3 Results and discussion

5.3.1 Impact of container size on MLSS settling

Container size does not play a significant role in settling of MLSS samples from the local reactor, when judged by the average variation in settling parameters listed in Table 5-3. The raw experimental data is tabulated in Table 11-5 and trends are displayed in Figure 11-2 to Figure 11-13 in Appendix D. For the average MLSS concentration of 4203 mg/ℓ, the average SVI, ISV, and supernatant turbidity from the three settling tests for the 1 ℓ and 2 ℓ cylinders differ by only 4 mℓ/g, 0.14 m/hr, and 2 FNU respectively. The smaller 1 ℓ cylinder samples heated up slightly faster, due to solar radiation, during the 30-minute settling tests. The faster sample heating in the 1 ℓ cylinder resulted in a small T_s difference of 0.3°C between the 1 ℓ and 2 ℓ cylinder samples after 30 minutes.

Table 5-3 Impact of container size on MLSS settling

Container [ℓ]	**T_{s30} [°C]**	**SVI [mℓ/g]**	**ISV [m/hr]**	**Turbidity [FNU]**
1	23.5	108	0.70	19
2	23.2	111	0.84	21
20	20.6	126	0.64	15

The settling results of the 20 ℓ sample differ slightly from the 1 ℓ and 2 ℓ samples. The limited area exposed to solar radiation in the large 20 ℓ container causes a slower T_s increase, compared to the 1 and 2 ℓ cylinders. At the lower T_s in the 20 ℓ container, the SVI is slightly higher and the ISV and supernatant turbidity slightly lower. The SVI, ISV, and turbidity change in the 20 ℓ container points directly towards the significant T_s impact on MLSS settleability. Wall effects and biofloc bridging effects are not present in the large 20 ℓ container. The reduced settleability (in terms of SVI and ISV) of the 20 ℓ sample is therefore related to T_s differences between small and large containers.

The SVI, ISV, and supernatant turbidity variations in the 1 ℓ, 2 ℓ, and 20 ℓ containers are small enough to accept that the 2 ℓ cylinder is suitable for the MLSS settling evaluations performed during the remainder of the experimental work. This verification ensures the container size is not a factor in 2 ℓ batch settling and 2 ℓ on-line settling test (based on the use of well-settling MLSS samples).

5.3.2 Impact of reactor zone on MLSS settling

Settling parameters are influenced differently as MLSS moves through the three BNR reactor zones. The SVI, ISV, and supernatant turbidity data is summarised in Table 11-3 in Appendix D, and illustrated in Figure 5-3. The SVI improves slightly after entering the aerobic reactor zone, but the ISV in essence stays unchanged through the three reactor zones. Supernatant turbidity reduces noticeably in all three reactor zones. This leads to a MLSS clarification improvement through successive zones in the BNR reactor.

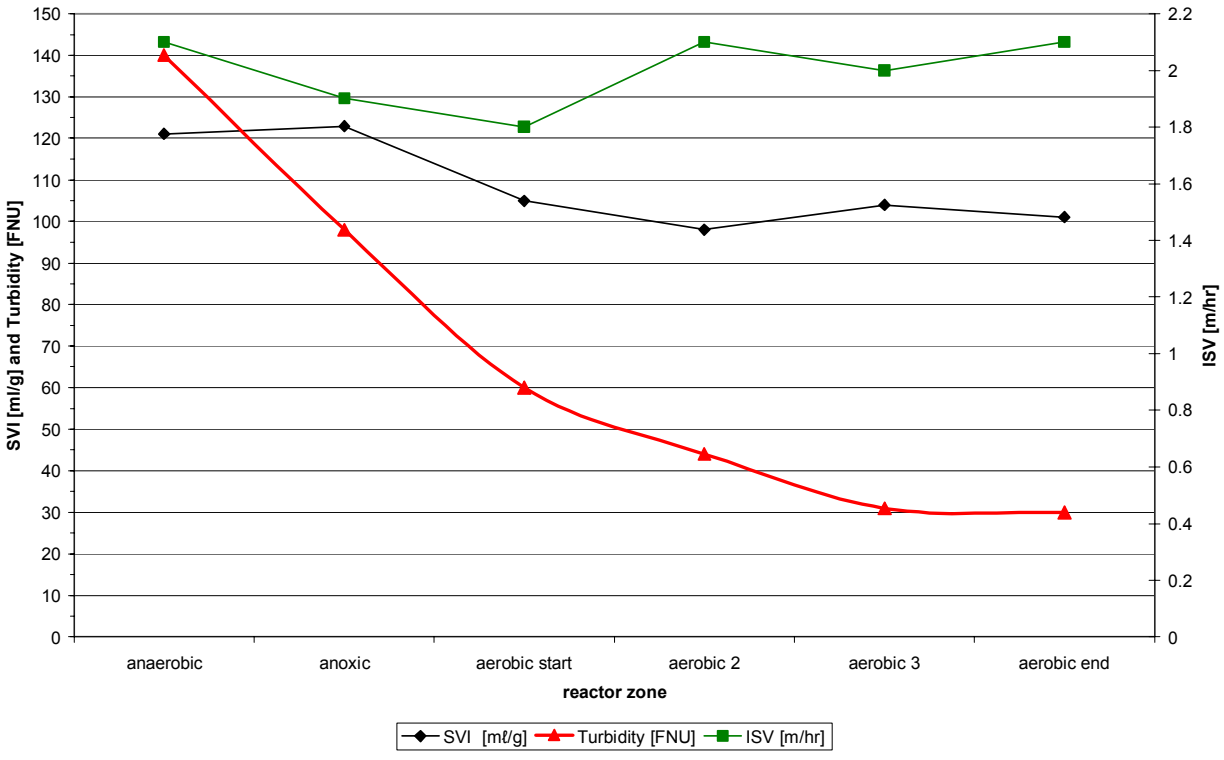

Figure 5-3 Settling parameters changes throughout three BNR reactor zones

The SVI improves from an average of 122 mℓ/g from the non-aerated anaerobic to anoxic zones, to an average of 102 mℓ/g in the four aerobic zones. The first aerobic section MLSS has a slightly higher SVI of 105 mℓ/g, against the average of 101 mℓ/g for the

MLSS in the other three aerobic sections. There is an immediate SVI improvement from the unaerated anoxic zone to the first aerobic zone. The standard deviation of SVI of 31 mℓ/g in the anaerobic to anoxic zones reduces to 11 mℓ/g in the four sections of the aerobic zone, which indicates a more stable SVI under aeration. The shift, from unaerated to aerated conditions, results in a small improvement in SVI, with an average SVI reduction measured at 19 mℓ/g.

ISV stays constant at an average of 2.0 m/hr from the anaerobic to anoxic zone, to 2.0 m/hr in the four sections of the aerobic zone. The average standard deviation of 0.6 m/hr stays constant throughout the reactor zones, for comparable settling velocity conditions in all reactor zones. The shift from unaerated to aerated conditions does not change the ISV significantly, with changes of about 0.3 m/hr measured between adjacent reactor zones.

Settled sewage mixes with RAS to create an anerobic zone at the reactor inlet, forming a MLSS with the highest supernatant turbidity of 140 FNU. This turbidity decreases by 42 FNU to 98 FNU in the anoxic zone, as the zone retention time and aerated a-recycle MLSS introduced into the anoxic zone appears to assist with MLSS flocculation to reduce supernatant turbidity. The turbidity reduces then by 38 FNU to 60 FNU in the first section of the aerobic zone. The turbidity reduction from the anaerobic zone to the start of the aerobic zone is 69%. The turbidity reduces subsequently slightly by 16 and 13 FNU in the second and third section of the aerobic zone, to 44 and 31 FNU respectively. No additional turbidity reduction is detected in the last section of the aerobic zone.

It appears that once a minimum aeration period is reached, extended aeration is not beneficial for further supernatant turbidity reduction. These results illustrate hydraulic residence time requirements in reactors and settling tanks, as simulated for MLSS settling by the 30-minute settling test duration. Ekama *et al.* (1997) found that an 1200 second (20 minute) flocculation duration is sufficient in full-scale settling tanks. The simulated 30-minute batch MLSS settling test is thus appropriate to determine the extent of supernatant clarification.

MLSS deflocculates when exposed to anaerobic conditions (Wilén *et al.*, 2000), as found in the anaerobic reactor zone. Reflocculation occurs relatively fast in the downstream reactor zones or under quiescent conditions in the stilling chamber of the secondary

settling tank. The SVI or settling velocity changes due to temperature variations in the different reactor zones is unknown from the available literature. This preliminary survey with 35 MLSS samples from six sections of a BNR reactor indicated the following changes to three MLSS settling parameters:

- SVI improves slightly in the aerobic reactor,
- ISV is relatively constant throughout reactor zones, and
- Supernatant turbidity reduces throughout BNR reactor zones.

5.3.3 Impact of container environment on MLSS settling

MLSS settling curves represent individual plant reactor conditions, and settling characteristics of MLSS is accordingly unique (Stypka, 1998). MLSS settling models, such as the Takács model (Takács *et al.*, 1991), require calibration with site-specific MLSS settling characteristics (Wilén, 2006) obtained from individual reactors.

The container environment plays a significant role in MLSS settling at an average MLSS concentration of 4203 mg/ℓ, as summarised in Table 5-4. The raw data is tabulated in Table 11-5 in Appendix D, and trends are displayed in Figure 11-2 to Figure 11-13 in Appendix D. The average SVI, ISV, and supernatant turbidity for three tests with the 1 ℓ and 2 ℓ cylinders differ significantly by about 50%, due to the placement of the cylinders in the sun or shade.

Table 5-4 Impact of container environment temperature on settling (T_r 19.6°C, T_a 17.9°C)

Cylinder [ℓ]	Position	T [°C] after 30 min	SVI [mℓ/g]	Change [mℓ/g/1°C]	ISV [m/hr]	change [m/hr/1°C]	Turbidity [FNU]	change [FNU/1°C]
1	Sun	23.5	108	N/A	0.70	N/A	19	N/A
	Shade	19.1	174	-15	0.04	0.15	14	1.2
2	Sun	23.2	111	N/A	0.84	N/A	21	N/A
	Shade	19.1	171	-14.6	0.44	0.10	14	1.7

SVI decreases with 1 ℓ and 2 ℓ samples are 15.0 mℓ/g and 14.6 mℓ/g per 1°C T_s increase respectively. The corresponding ISV increases are 0.15 m/hr and 0.10 m/hr per 1°C T_s

increase respectively. The corresponding supernatant turbidity increases are 1.2 FNU and 1.7 FNU per 1°C T_s increase respectively. The average SVI decrease, the ISV increase, and the supernatant turbidity increase are therefore 14.8 mℓ/g, 0.12 m/hr, and 1.42 FNU per 1°C T_s increase respectively.

Local effects of solar radiation on sample placements in the shade or direct sunlight result in a temperature difference of about 4.3°C over 30 minutes. This large T_s variation confirms the important effect of solar radiation intensity on water bodies, as observed by Tadesse *et al*. (2004). The large variations in excess of 50% in SVI, ISV, and supernatant turbidity indicate the importance of sample environmental conditions control, as well as temperature compensation and recordings before and during batch MLSS settling tests.

5.4 Summary

Several aspects of batch MLSS settling tests procedures influence results. The three aspects of settling procedures evaluated in this study consist of (i) container size, (ii) reactor zone sample origin, and (iii) container environment.

- Container size (1 ℓ, 2 ℓ or20 ℓ) does not change the SVI, ISV, or supernatant turbidity of the plant specific MLSS samples significantly.

- MLSS samples from the three BNR reactor zones do not exhibit large variations in SVI or ISV, but the clarified supernatant turbidity improves throughout successive BNR reactor zones.

- Temperature-dependent MLSS settling variations are not linear over an extended T_s range. A larger MLSS settleability deterioration change is evident at lower T_s.

- Temperature variations during sample handling have significant impacts on MLSS settling. An average SVI decrease of 14.8 mℓ/g per 1°C T_s increase, an ISV increase of 0.12 m/hr per 1°C T_s increase, combined with a supernatant turbidity increase of 1.7 FNU per 1°C T_s increase, were measured during 30-minute MLSS batch settling tests, at a total T_s variation of about 4.3°C.

- No temperature dependent settling trends are identified across the BNR reactor from these standard MLSS batch settling tests. This indicates the insensitivity of conventional settling equipment and traditional methods to attempt to perform temperature dependent batch MLSS settling tests over small operational T_r ranges.

5.5 Conclusions

The general conclusions to summarise experimental results are as follows:

- Temperature has a significant impact on MLSS settling, with a SVI decrease of 14.8 mℓ/g per 1°C T_s increase, an ISV increase of 0.12 m/hr per 1°C T_s increase, combined with a clarified supernatant turbidity increase of 1.7 FNU per 1°C T_s increase. At higher temperatures within the operational T_s range, MLSS settling improves, and supernatant clarification deteriorates.

- Temperature dependent MLSS settling variations are not linear, with larger MLSS settleability deterioration evident at lower temperatures, when compared to small MLSS settleability changes at higher temperatures outside the operational T_s range.

- There is an immediate, but relatively small, improvement in MLSS settleability, in terms of SVI, when anaerobic MLSS is aerated.

- There is a continuous improvement in supernatant clarification, according to the turbidity reduction, when anaerobic MLSS transfers through successive reactor zones. Aeration results in supernatant turbidity reduction until a mimimum turbidity is reached.

- Existing conventional batch settling equipment and traditional basic procedures are not suitable to effortlessly identify temperature dependent MLSS settling changes over small operational T_r ranges.

The significant effects of short-term temperature changes on batch MLSS settling test results creates the need for more advanced MLSS settling monitoring techniques. On-line MLSS settling is such a technique, where temperature compensation is incorporated in the settling sampling and test method.

6 ON-LINE MLSS SETTLING EVALUATION

On-line MLSS settling profiles are evaluated in this chapter. Profiles are obtained from an automated MLSS settling meter to calculate temperature and MLSS concentration-based settling parameters. The improved MLSS settling models illustrate the effects of including short-term temperature fluctuations in the determination of settling parameters.

6.1 Background

The capacity and performance of a secondary settling tank relates to the velocity at which MLSS separates and settles to the bottom of the tank (Jeyanayagam *et al*., 2006). MLSS concentration and MLSS settling velocity measurements are thus required to perform a batch MLSS settleability evaluation. On-line instrumentation is available to perform these manual measurements on an automated basis. Gernaey *et al*. (1998) consider the development and use of such on-line MLSS settling meters as a major improvement on batch MLSS settleability tests.

MLSS concentration is the main factor that contributes to variations in the MLSS settling process (Reardon, 2005). Numerous additional settleability factors are summarised for reference purposes in alphabetical order in Table 11-7 to Table 11-12 in Appendix G. These factors create suitable conditions for the formation of a well-settling MLSS. The most essential factors include a sufficient sludge age in the BNR reactor, combined with suitable DO concentrations in the different reactor zones, as well as a wastewater feed containing adequate substrates (De Clercq *et al*., 2007).

Temperature is a settleability factor that affects several aspects of MLSS settling (Morgan-Sagastume and Allen, 2003). Temperature modifies water density and water viscosity (Clements, 1976), as well as the surface and composition characteristics of the individual bioflocs (Gerardi, 2002). These temperature-based MLSS settling changes are highly variable, due to operational T_r variations. The short-term T_r variations follow diurnal T_a fluctuations, while long-term T_r variations follow seasonal T_a fluctuations (Wahlberg *et al.*, 1996).

On-line MLSS settling meters are ideally suited to monitor and collect MLSS settling data over these diurnal T_r fluctuations. There are three main developments reported on the

implementation of automated MLSS settling equipment. (i) One of the first reported MLSS settling meters was developed in Japan (Sekine *et al.*, 1989) in the late 1980s for batch settling tests. This MLSS settling meter is able to measure SVI, compression velocity, as well as ISV. (ii) A second unit was developed in Belgium (Vanderhasselt *et al.*, 1999b) in the 1990s for on-line MLSS settling tests. This settling meter includes a stirrer to measure SSVI. Vanrolleghem *et al.* (1996) reports that this meter is designed with a sample dilution function to measure DSVI. (iii) Wahlberg (2004) developed a settling meter that is patented as an apparatus, as well as an integrated method, to measure and manipulate MLSS settling, compression and flocculating characteristics.

Simon *et al.* (2005) and Lynnggaard-Jensen and Lading (2006) recently described a novel settling meter sensor that consists of a sample chamber intended for direct submersion into a reactor. This sensor is equipped with an array camera and photo sensor to measure the MLSS settling interface over 30 minutes. These reports indicate that substantial research and development is directed to automate aspects of the traditional batch MLSS settling test.

The aim of this chapter is to model temperature dependent MLSS settling parameters. The parameters are obtained from semi-continuous MLSS settling profiles that are generated during diurnal T_r fluctuations with the use of an automated on-line MLSS settling meter.

6.2 Materials and methods

6.2.1 Experimental approach

On-line MLSS settling tests are performed at a full-scale BNR reactor outlet. Van Huyssteen *et al*. (1990) describe this plant in some detail. The on-line settling tests are required to confirm that the range of temperature related full-scale MLSS settling changes are comparable to settling parameter changes identified during the preliminary batch MLSS settling tests, as reported in Chapter 5.

The automated on-line MLSS settling meter generates about 40 successive MLSS settling profiles per 24-hour day. The settling data and profiles, in electronic format, are used to calculate settling parameters. A statistical computer software program evaluates these parameter correlations to obtain temperature dependent MLSS settling models. A

practical approach is therefore provided to improve the reliability of MLSS settling parameters, as effects of short-term temperature variations before and during MLSS settling tests can be virtually eliminated.

6.2.2 MLSS settling meter configuration

The custom-built MLSS settling meter automates the monitoring and recording of batch MLSS settling tests. The settling meter monitoring method is based on a vertical moving single point infrared light detector that consists of a light source and receiver. The light detector follows the descending liquid / MLSS interface along a transparent cylinder filled with MLSS. The program logic controller (PLC) records the height of the light detector in electronic format during the MLSS settling period, thereby generating a settling profile.

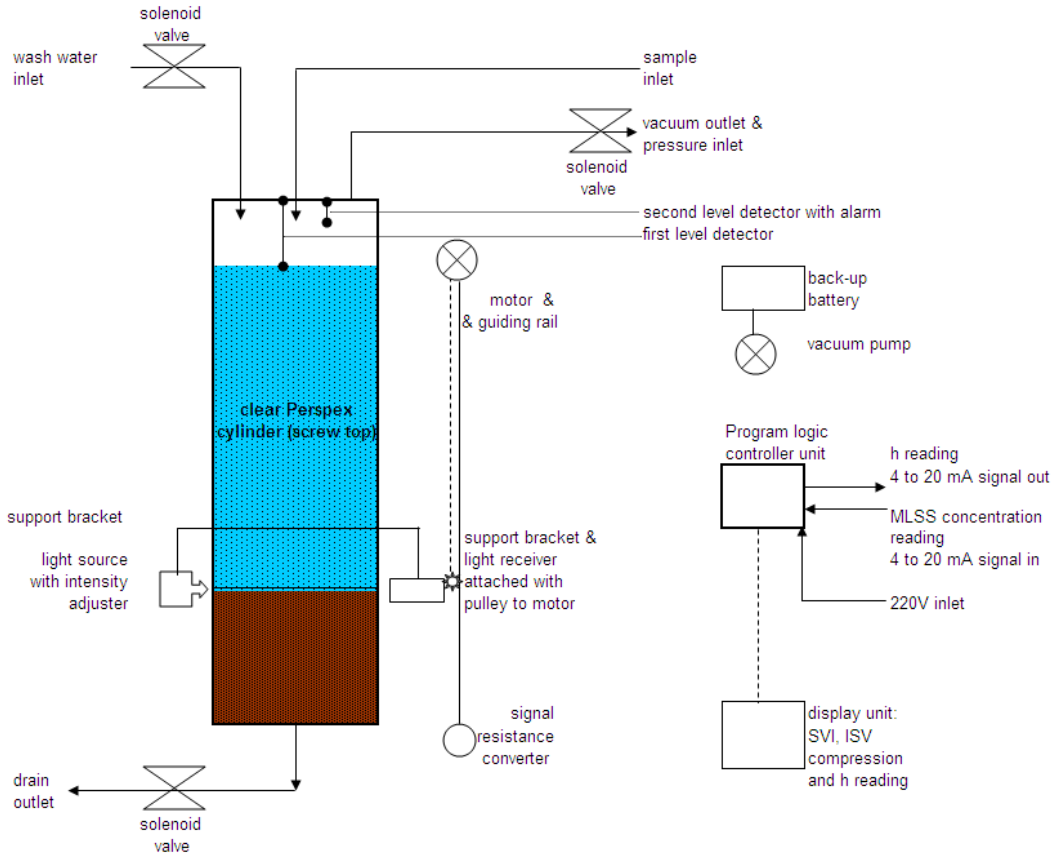

Figure 6-1 Schematic diagram of main components of the MLSS settling meter

Three requirements of the MLSS settling meter are: (i) to obtain MLSS samples without subjecting bioflocs to excessive turbulence, (ii) to trend successive 30-minute MLSS

settling profiles together with T_r and MLSS concentration data, and (iii) to operate fully automated and without supervision.

Figure 6-1 illustrates the main components of the MLSS settling meter. A vacuum driven sample suction system transfers the MLSS sample from the reactor basin into the cylinder. The vacuum system also pressurises the cylinder after each settling test to drain the cylinder, and to flush out any stagnant MLSS sample trapped in the transfer pipe. The vacuum system ensures the MLSS sample is not exposed to excessive pump shear during sample transfer. A wide cylinder is used to prevent or reduce wall effects during settling. The clear Perspex cylinder has a working volume of 2 ℓ, with a height of 360.9 mm, an internal diameter of 84.0 mm, and a wall thickness of 3.5 mm.

The MLSS sample transfer is rapid and the cylinder fills up within a few seconds. The MLSS sample discharge into the cylinder creates enough turbulence to ensure the sample mixes homogenously. The settling test starts immediately after a maximum level detector stops the sample transfer. The scanner moves downward to follow the settling liquid / MLSS interface level during the 30-minute test duration. The light sensor activates almost instantaneously as the MLSS settles, due to the scanner light source signal that the detector receives through the transparent clarified supernatant. The sensor stops moving down once the scanner light source signal is lost, due to the opaque settled MLSS. The sensor moves downward in about 4 mm increments, which is the minimum distance that the geared drive unit of the sensor can move.

The PLC records the MLSS interface level after each minute of the 30-minute settling period. The PLC calculates the initial settling velocity (minutes 2 to 5 of the 30-minute test) and the SVI. These parameter values appear on a digital display unit after each settling cycle. The settling meter has a manual termination function to cancel a test and to restart the complete settling cycle.

The settling meter is relatively mobile and simple to commission. The meter start-up requires a 220 V power source, a potable wash water supply, a 4 to 20 mA signal input from the reactor MLSS concentration meter, as well as a MLSS sample source. The MLSS concentration reading is not essential for the MLSS settling meter operation, as it is only used for the SVI display and SVI calculation. The settling meter and components

are installed in a fully enclosed weatherproof cabinet, to eliminate or reduce meteorological effects, such as wind, rain, solar radiation, and T_a changes. Photograph 1 in Appendix F shows the general arrangement of the MLSS settling meter components. The automated operation sequence to create one MLSS settling profile consists of the following three steps:

Step 1: MLSS sample preparation

- cylinder drain valve opens,
- cylinder chamber pressurises to force out previous MLSS sample through bottom drain and to flush top MLSS sample inlet line, adjustable duration of 5 seconds,
- potable wash water cleaning cycle to spray inner cylinder walls, adjustable duration 4 seconds,
- cylinder chamber pressurises to force out wash water through bottom drain, adjustable duration 5 seconds,
- cylinder drain valve closes,
- cylinder chamber under vacuum to extract MLSS sample from reactor basin into cylinder,
- vacuum stops when cylinder maximum level sensor at 2 ℓ capacity is detected,
- external initial reactor MLSS concentration reading obtained for SVI calculation, and
- external logger T_r is recorded.

Step 2: MLSS settling test

- 30 minute counter starts,
- MLSS settling interface height is recorded every minute for 30 minutes according to level of light detector,
- height reading capture at 120 seconds,
- height reading capture at 300 seconds, PLC calculates, displays ISV (2 to 5 minutes),
- height reading capture at 1500 seconds,
- height reading capture at 1790 seconds, PLC calculates, displays compression velocity (25 to 30 minutes), and
- final height capture according to light detector level at 30 minutes, PLC calculates, displays SVI.

Step 3: MLSS sample removal

- light detector moves upwards to the start position at maximum cylinder height level, and
- step 1 restarts after a total of 46 minutes (16-minute adjustable period between tests), except if the manual override function is turned on at any stage to return to start of step 1.

A two-channel data logger (Microlog Plus; Fourier, 2007) captures the settling meter height profiles. The logger data is recorded in a Microsoft Excel compatible format to ensure manual download to a computer.

6.2.3 MLSS settling meter velocity data collection method

The settled MLSS height (h) variations over 30-minute settling test duration are obtained from the original MLSS settling profiles, as illustrated in Figure 6-2. The stage 1 lag or reflocculation time, stage 2 ZSV or u_max, stage 3 transition, and stage 4 compression are indicated on successive settling profiles.

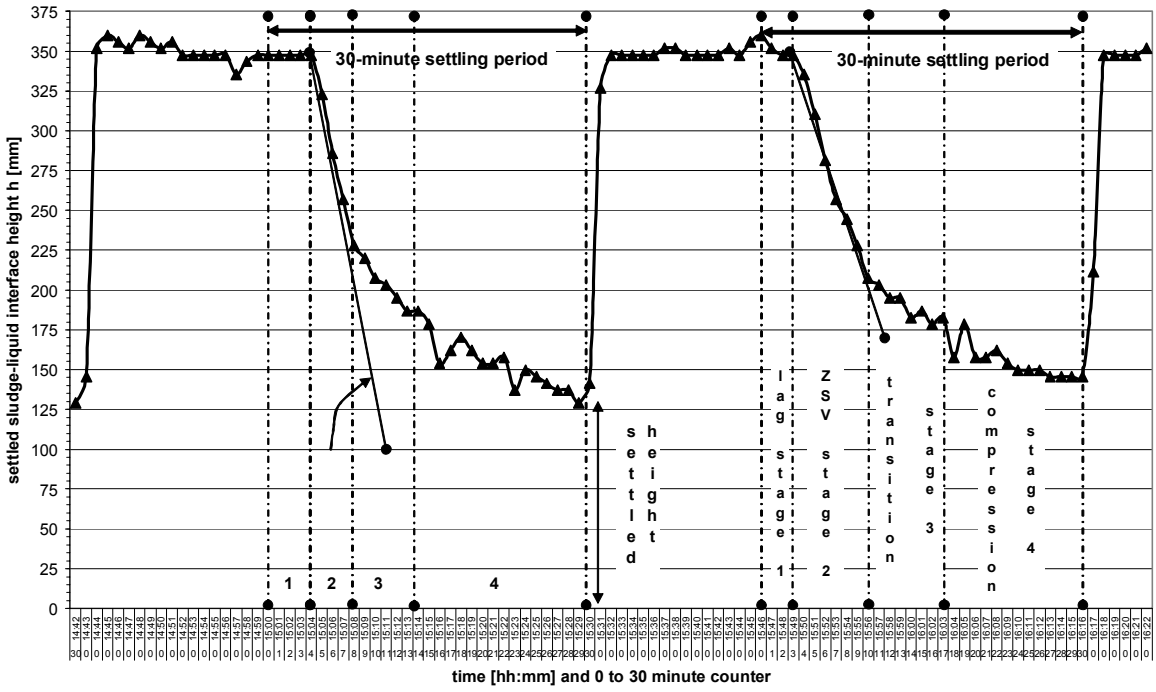

Figure 6-2 Two consecutive on-line MLSS settling profiles recorded by the settling meter

The MLSS settling parameters are computed from these settling profiles with the use of a Microsoft Excel spreadsheet as follows:

- lag time before settling of liquid / MLSS interface starts (stage 1),
- ISV from period 2 to 5 minutes of MLSS settling,
- u_max from the linear negative slope (stage 2),
- t_umax from when u_max commences (start of stage 2),
- SV_{30} from the settled MLSS height after 30 minutes (end of stage 4), and six incremental 5-minute MLSS settling velocities over 30 minutes: u1, u2, u3, u4, u5, u6.

6.2.4 MLSS settling meter velocity data collection boundaries

The on-line MLSS meter generated 85 settling profiles for the full-scale plant. The experimental data range boundaries for these profiles are listed in Table 6-1. The MLSS concentration and T_r variations at the full-scale plant are recorded from 4489 to 4923 mgSS/ℓ, and from 17.2 to 19.0°C respectively.

Table 6-1 Experimental data range for on-line MLSS settling evaluation

Parameter	Full-scale reactor condition
n	85
Minimum T_r [°C]	17.2
Maximum T_r [°C]	19.0
Minimum MLSS concentration [mg/ℓ]	4489
Maximum MLSS concentration [mg/ℓ]	4923

6.2.5 Data presentation

6.2.5.1 Data logger transfer and calculations

A data logger (Microlog Plus; Fourier, 2007) equipped with an internal thermometer measures and records T_r. The logger has an external 4 to 20 mA signal input facility that is used to store the settling meter h data. A similar data logger is used to record T_r from the built-in thermometer of the DO concentration meter (ATI Model B15\60; ATI, 2007). An additional data logger (Alog MCS131LCD; MC Systems, 2007) stores the on-line

data from the DO and MLSS concentration meters. The data collection proceeds as follows:

- The DO concentration meter data logger produces a data table of readings of date [dd-mm-yyyy], time [hh:mm] in 5 minute increments, and DO concentration [mg/ℓ] in 0.1 mg/ℓ increments. The data tables are transferred into Excel spreadsheets.
- The MLSS concentration meter data logger produces a data table of readings of date [dd-mm-yyyy], time [hh:mm] in 5 minute increments, and MLSS concentration [mg/ℓ] in 0.1 mg/ℓ increments. The data tables are transferred into Excel spreadsheets.
- The MLSS settling meter data logger produces a data table of readings of date [dd-mm-yyyy], time [hh:mm:ss] in 1 minute increments, and height [mm] in 0.1 mm increments. The data tables are transferred into Excel spreadsheets.
- The thermometers data produces data tables of readings of date [dd-mm-yyyy], time [hh:mm] in 5 minute increments, T_a from the internal ambient temperature sensor in 0.3°C increments and T_r from the DO concentration meter temperature sensor [°C] in 0.3°C increments. The data tables are transferred into Excel spreadsheets.

The Excel spreadsheet containing the settling meter height data is the reference sheet for all calculations. An example of a settling data graph is provided in Figure 11-14 in Appendix E. Data in the spreadsheet is not filtered to remove noise. Bergh (1996) describes experimental noise as fluctuations in measurements that originate from the process or measuring devices used.

The cylinder height readings [mm] are converted to cylinder volume values [mℓ]. The DO and T_r readings are averaged over each 30-minute settling period, and the initial MLSS concentration reading is used to calculate SVI. The MLSS settling profile over 30 minutes is used to calculate the 11 MLSS settling parameters: SVI [mℓ/g], u_max [m/hr], u_ave [m/hr], t_umax [minute], h [mm] and the six incremental u1 to u6 five-minute settling velocities [m/hr].

The reference Microsoft Excel spreadsheet is used to list the date, time, DO concentration, MLSS concentration, SV_{30}, SVI, t_umax, u_max, u_ave, h, and u1 to u6. The two dependent variables, MLSS concentration and T_r, are transferred together with the 11 settling parameters into the DataFit (2005) statistical computer program.

6.2.5.2 Empirical settling correlations and statistical comparisons

The MLSS settling data is used to generate 2-D best-fit correlations between the MLSS concentration and the 11 MLSS settling parameters. The same settling data is then used to generate 3-D best-fit correlations with MLSS concentration, T_r, and the 11 MLSS settling parameters. To evaluate the impact of T_r inclusion, the improvement in correlations can be statistically determined by comparing R^2-values. R^2 is the most widespread coefficient used to assess MLSS settling models (Ozinsky and Ekama, 1995).

There are 298 single independent 2-D regression models and 242 3-D non-linear regression models pre-defined in DataFit (2005). These pre-defined models allocate best-fit correlations for the settling data according to R^2-values. This automatic ranking function of DataFit identifies the best-fit correlations.

The DataFit package generates 3-D plots of the regression models, where the dependent variables are allocated to the x_1- and x_2-axes, and the response variables to the y-axis. In the graphical display of the non-linear regressions, bullets above and below the surfaces indicate the data points, and the surfaces with colour bands indicate the regression result ranges. The built-in regression analysis function of Microsoft Excel analyzes the rest of the experimental MLSS settling data.

6.3 Results and discussion

The mathematical relationships between settleability parameters are approximated as basic polynomial functions, to show trends that adequately describe MLSS settling behaviour. The on-line MLSS settling results are presented in the following sections:

- settling parameters diurnal profiles (h, MLSS concentration, SVI)
- settling parameters best-fit model
  - dependent variables: MLSS concentration and T_r
  - response variables: SVI, u_max, and t_umax
- settling parameter model correlations (SVI with u_max and t_umax)
- settling parameters simplified models
  - dependent variables: MLSS concentration and T_r
  - response variables: SVI, u_max, t_umax, u_ave, h, u1, u2, u3, u4, u5, u6

6.3.1 h and T_r diurnal variation

The recorded data points and fitted trends for the diurnal T_r and settled MLSS height variations are shown in Figure 6-3. The x_1-axis indicates the 24-hour diurnal period, the primary y_1-axis indicates T_r, and the secondary y_2-axis indicates the on-line MLSS settling meter h reading.

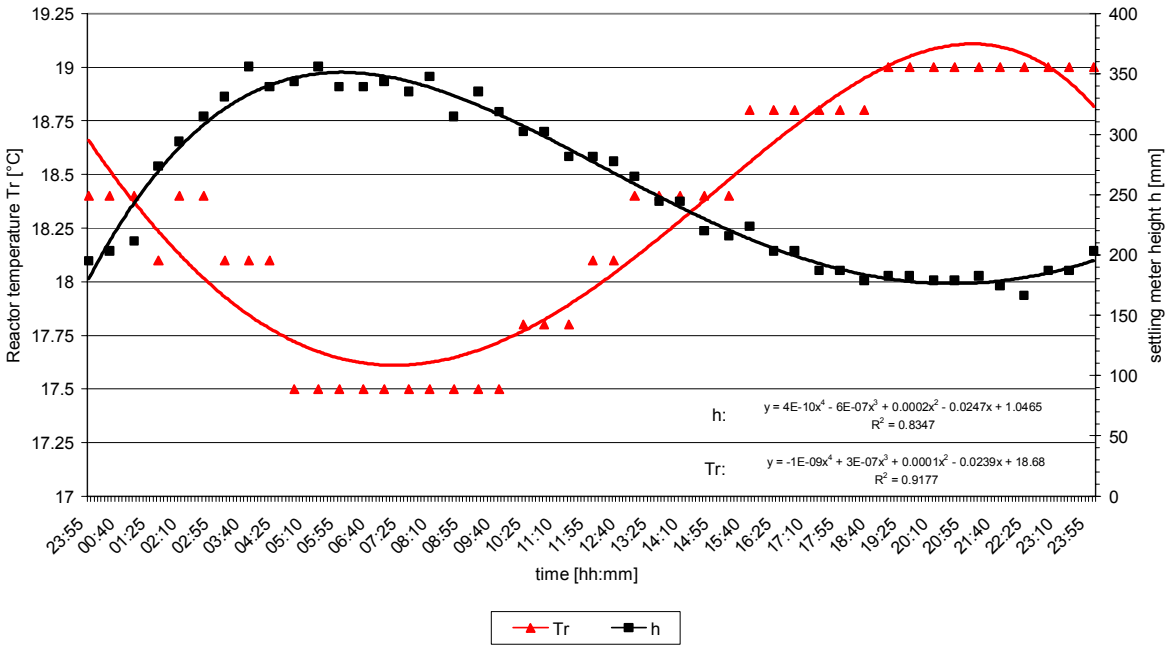

Figure 6-3 Data and fitted curves of temporal variations in T_r and h

The full-scale plant T_r fluctuated by about 1.5°C per typical day in spring. The T_r profile changed from 17.5 to 19.0°C, and the h profile changed from about 350 to 170 mm, as shown in Figure 6-3. These T_r and h profiles follow sinusoidal wave profiles, as represented by the fitted curves with R^2 of 0.92 and 0.83 respectively. From the on-line MLSS settling tests, the MLSS settling meter height reading illustrated the inverse relationship between T_r and the 30-minute settled MLSS height in a settling test cylinder.

6.3.2 MLSS concentration and T_r diurnal variation

The recorded data points and fitted trends for the diurnal T_r and MLSS concentration variations for the full-scale plant are shown in Figure 6-4. The x_1-axis indicates the 24-hour diurnal period, the primary y_1-axis indicates T_r and the secondary y_2-axis indicates the on-line MLSS concentration reading. Two 2-day profiles, with T_r and MLSS concentration correlations R^2 of 0.91 and 0.90 respectively, are provided in Figure 11-16 in Appendix D for reference purposes.

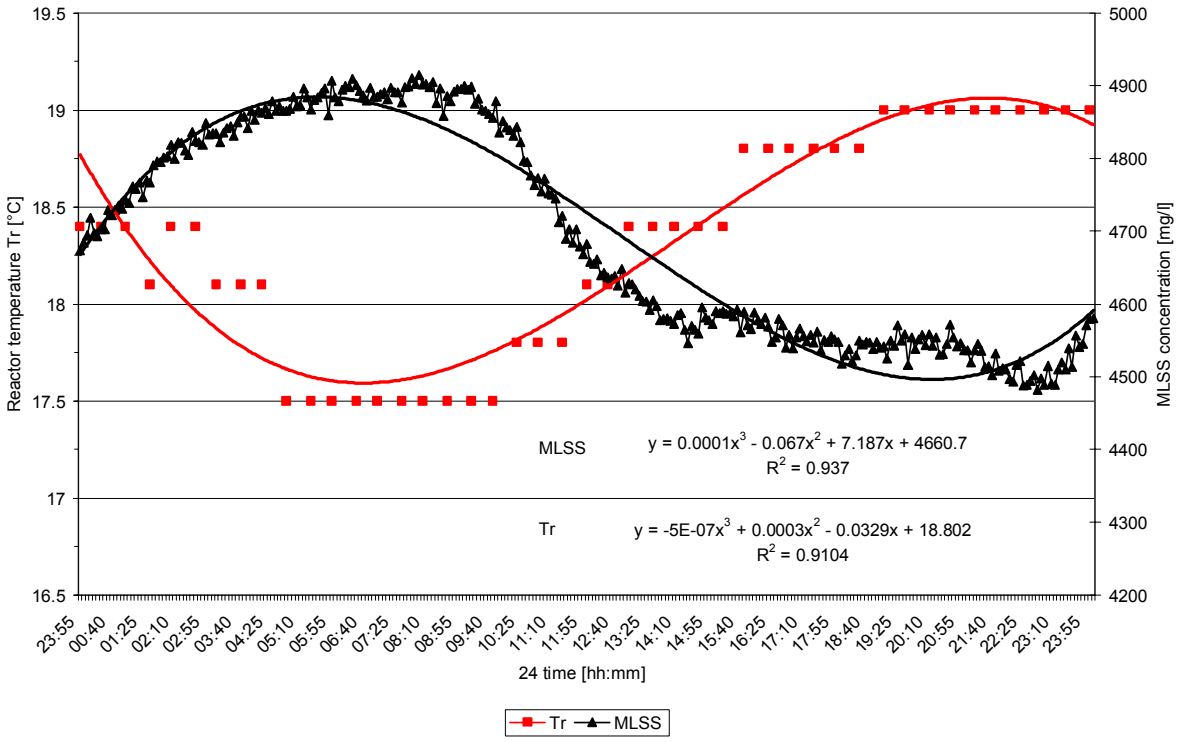

Figure 6-4 Data and fitted curves of temporal variations in T_r and MLSS concentration

The full-scale plant average MLSS concentration varies by about 400 mg/ℓ per day. The diurnal MLSS loading variations, originating from the plant and reactor inflow, as well as the secondary settling tank RAS flow, cause MLSS concentration variations (Otterpohl and Freund, 1992). This MLSS concentration profile was relatively smooth over the 24-hour period, as shown in Figure 6-4. The T_r and MLSS concentration profiles follow a sinusoidal wave profile, as represented by fitted curves with R^2 of 0.92 and 0.94 respectively.

6.3.3 SVI and T_r diurnal variation

The calculated SVI, recorded data points for the diurnal T_r, and fitted trends for the full-scale plant, are shown in Figure 6-5. The x_1-axis indicates the 24-hour diurnal period, the primary y_1-axis indicates T_r, and the secondary y_2-axis indicates the calculated SVI reading. Two 2-day profiles, with SVI and T_r correlations R^2 of 0.92 and 0.91 respectively, are provided in Figure 11-17 in Appendix D for reference purposes.

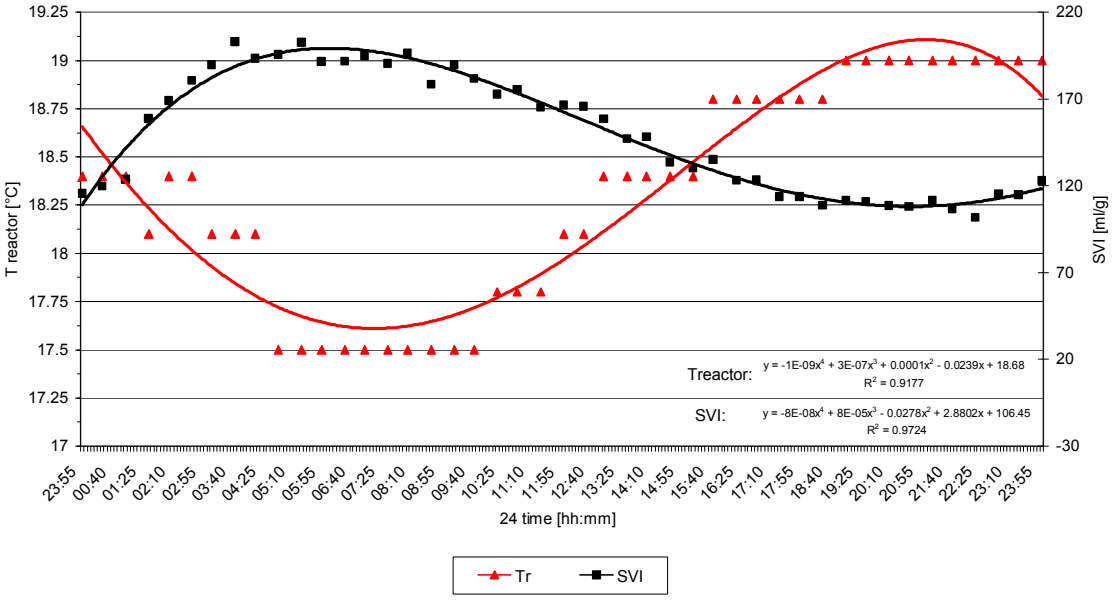

Figure 6-5 Data and fitted curves of temporal variations in T_r and SVI

The full-scale plant average SVI varies by about 100 mℓ/g per day. This variation was caused by the diurnal MLSS concentration and T_r fluctuation. The SVI profile was relatively smooth over a daily 24-hour period, as shown in Figure 6-5. The T_r and SVI trends follow sinusoidal wave profiles, as represented by fitted curves with R^2 of 0.92 and 0.97 respectively.

Two 2-day profiles, with SVI and MLSS concentration correlations R^2 of 0.92 and 0.90 respectively, are provided in Figure 11-18 in Appendix D for reference purposes.

6.3.4 Model fitting: SVI dependence on MLSS concentration and T_r

The SVI dependence on MLSS concentration and T_r is statistically evaluated with individual and combined correlations in 2- and 3-D models.

6.3.4.1 SVI link to MLSS concentration

The recorded data points and a fitted trend for the on-line MLSS concentration and calculated SVI are shown in Figure 6-6. The x-axis indicates MLSS concentration, and the y-axis indicates SVI. The best-fit curve for SVI related to MLSS concentration from full-scale data is represented by a polynomial with a R^2 of 0.69, as shown in Figure 6-6.

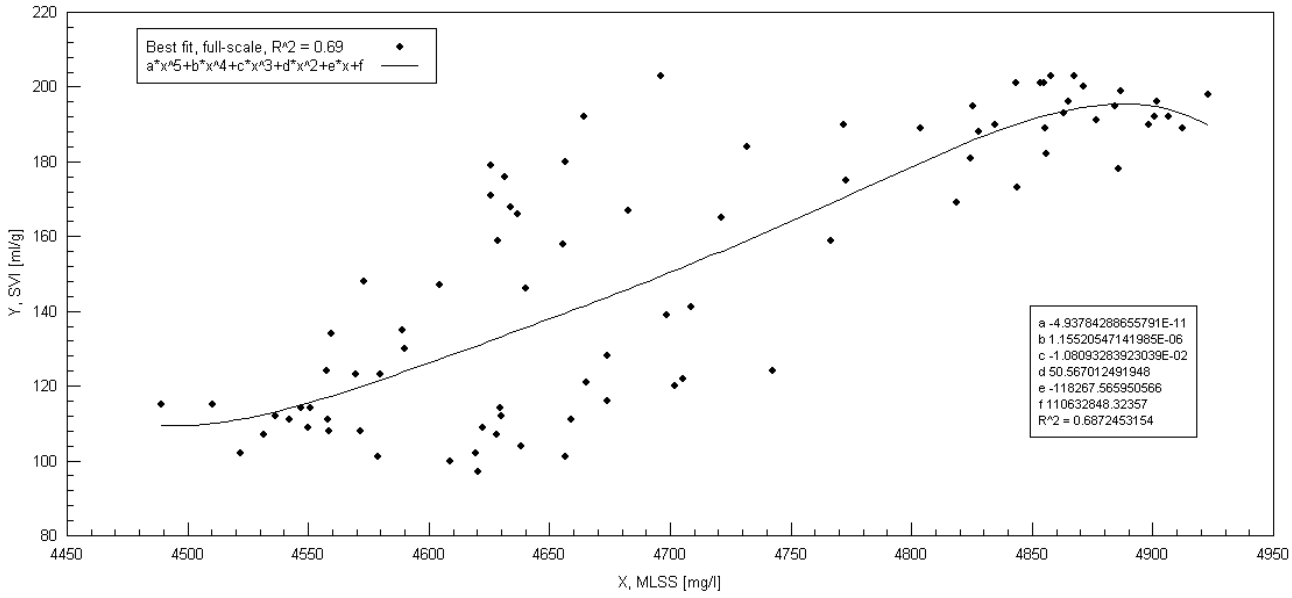

Figure 6-6 SVI related to MLSS concentration

The direct relationship between SVI as the response variable and MLSS concentration as the dependent variable is confirmed by the polynomial, since SVI increases according to the best-fit curve as MLSS concentration increases. The calculated SVI data scatter was visible from 97 to 203 mℓ/g throughout the MLSS range of 4489 to 4923 mg/ℓ. The data scatter is in agreement with earlier observations of experimental MLSS settling data and calculated SVI ranges, as presented in models by Daigger and Roper (1985) and Catunda and Van Haandel (1992). There are therefore other significant factors present that are not incorporated in the traditional SVI regression models based only on MLSS concentration. Ambient and reactor temperature fluctuations, and the related change in sample temperature, are such factors that can account for some of the scatter in SVI data.

6.3.4.2 SVI link to T_r

The recorded data points and a fitted trend for the on-line T_r and calculated SVI are shown in Figure 6-7. The x-axis and the y-axis indicate the T_r and SVI respectively. The best-fit curve for SVI related to T_r for full-scale plant data is represented by a 6^{th} order polynomial, based on a very low R^2 of only 0.38.

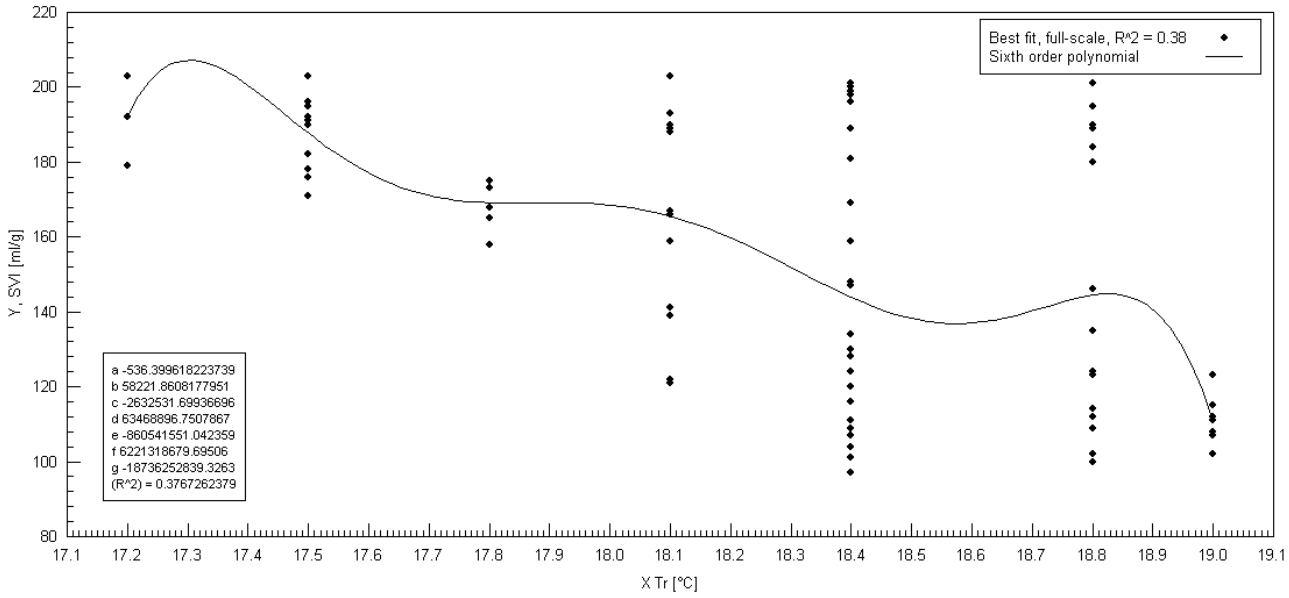

Figure 6-7 SVI data scatter according to T_r variation

A basic inverse relationship between SVI as the response variable and T_r as the dependent variable is visible in Figure 6-7, as SVI decreases as T_r increases. The large experimental SVI data scatter was present throughout the fixed T_r range, since the T_r data logger only recorded in 0.3°C increments.

This large data scatter indicates that the SVI data cannot be correlated with only T_r as a single dependent variable. The MLSS concentration is required as a second dependent variable in a 3-D model to reduce the data scatter and to obtain a best-fit correlation for the experimental and calculated data.

6.3.4.3 SVI link to MLSS concentration and T_r

The recorded data points and fitted correlation for the on-line MLSS concentration, the T_r, and the calculated SVI are shown in Figure 6-8. The x_1-, x_2- and y-axis represent MLSS concentration, T_r, and SVI respectively. The best-fit curve for SVI related to MLSS concentration and T_r for full-scale plant data is represented on Figure 6-8 by a polynomial with a R^2 of 0.84.

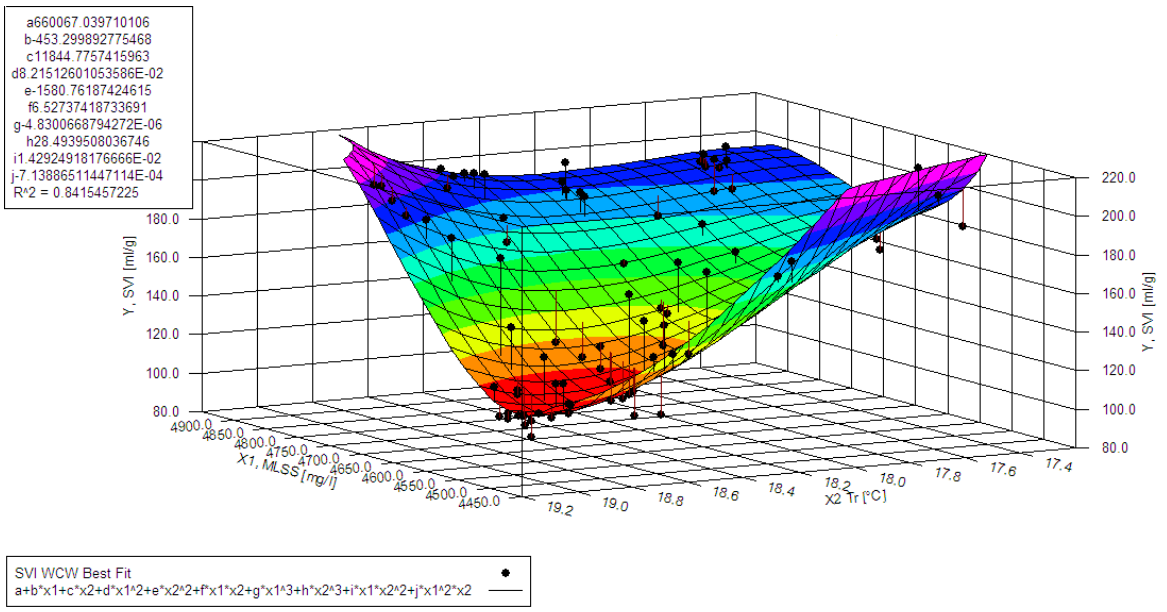

Figure 6-8 SVI related to MLSS concentration and T_r

The temperature impact on settling is demonstrated by the improved curve fitting when T_r data is included in the full-scale plant SVI evaluation. Figure 6-8 illustrates the relationship between SVI as the response variable, with MLSS concentration and T_r as the dependent variables. The SVI response, after a variation in either or both the MLSS concentration and T_r, can be predicted from Figure 6-8.

SVI increases from 97 towards 203 mℓ/g as the MLSS concentration increases from 4489 to 4923 mg/ℓ and the T_r decreases from 19.0 to 17.2°C. The ideal settling condition of the lowest SVI of 97 mℓ/g is obtained at the lowest MLSS concentration and the highest T_r. The inclusion of T_r in SVI correlations improves the curve fitting by a R^2 value of 0.15, from 0.69 to 0.84.

6.3.5 Model fitting: u_max dependence on MLSS concentration and T_r

The u_max dependence on MLSS concentration and T_r is statistically evaluated with individual and combined correlations in 2- and 3-D models.

6.3.5.1 u_max link to MLSS concentration

The recorded data points and a fitted trend for the full-scale on-line MLSS concentration and calculated u_max are shown in Figure 6-9. The x_1-axis indicates MLSS concentration and the y-axis indicates u_max. The best-fit curve for u_max related to MLSS concentration from full-scale data is represented by a polynomial with a R^2 of 0.58, as shown in Figure 6-9.

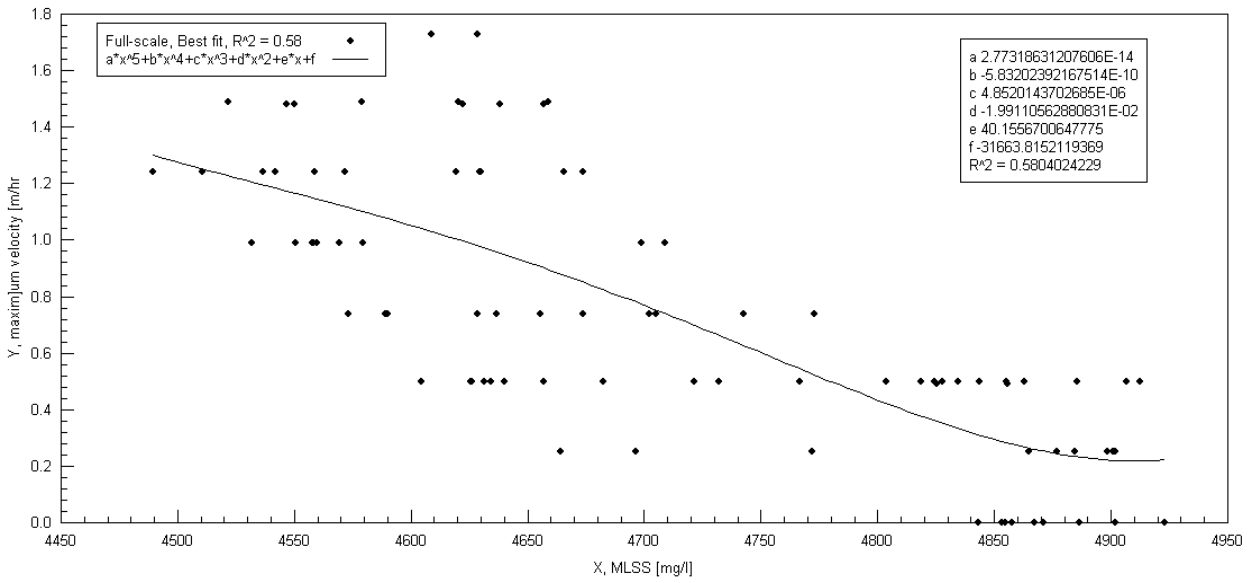

Figure 6-9 u_max related to MLSS concentration

The inverse relationship between u_max as the response variable and MLSS concentration as the dependent variable is confirmed, since u_max decreases according to the best-fit curve as MLSS concentration increases. The experimental u_max data scatter is visible from 0 to 1.73 m/hr throughout the MLSS range of 4489 to 4923 mg/ℓ.

6.3.5.2 u_max link to T_r

The recorded data points and a fitted trend for the on-line T_r and calculated u_max are shown in Figure 6-10. The x_1-axis indicates the T_r and the y-axis indicates the u_max. The best-fit curve for u_max related to T_r from the full-scale plant data is represented by a polynomial with a very low R^2 of only 0.26.

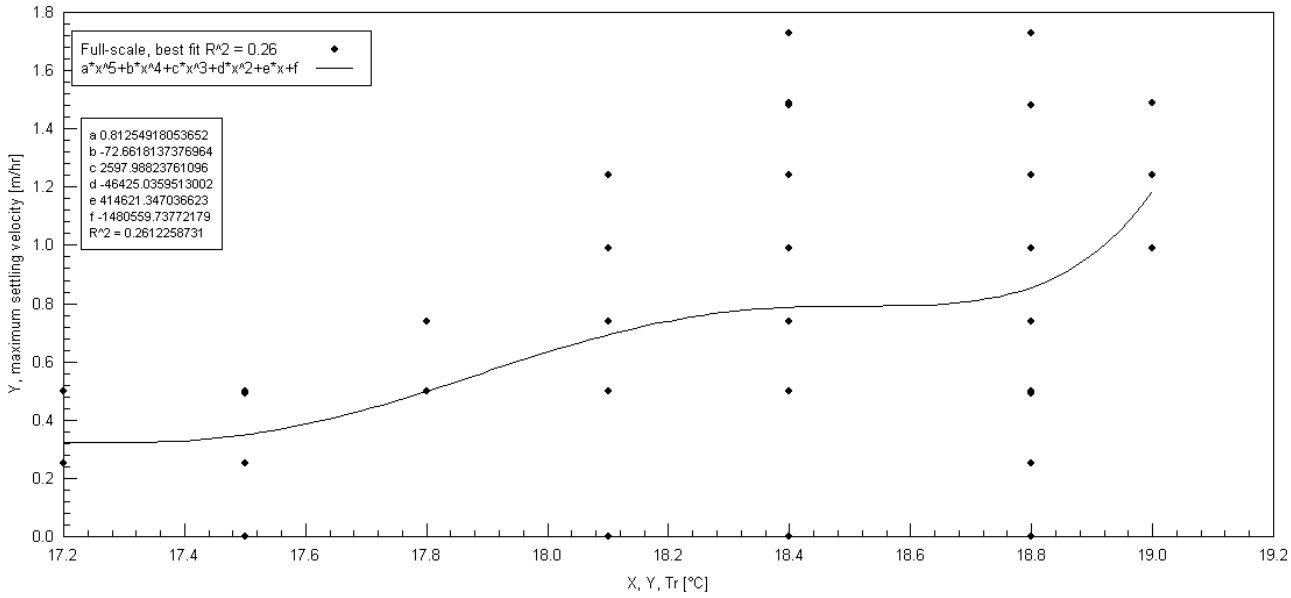

Figure 6-10 u_max data scatter according to T_r variation

A basic correlation between u_max as the response variable and T_r as the dependent variable is visible, as u_max increases according to the best-fit curve as T_r increases. The large field of experimental u_max data scatter is visible throughout the T_r range increments, since the T_r data logger only recorded in 0.3°C increments.

The large data scatter indicates that the u_max data cannot be correlated with only T_r as a single dependent variable. The MLSS concentration is required as a second dependent variable in a 3-D model to reduce the data scatter and to obtain a best-fit correlation for the experimental and calculated data.

6.3.5.3 u_max link to MLSS concentration and T_r

The recorded data points and fitted correlation for the on-line MLSS concentration, T_r, and calculated u_max are shown in Figure 6-11. The x_1-, x_2- and y-axis represent MLSS concentration, T_r, and u_max respectively. The best-fit curve for u_max related to MLSS concentration and T_r for full-scale plant data was represented on Figure 6-11 by a polynomial with a R^2 of 0.70.

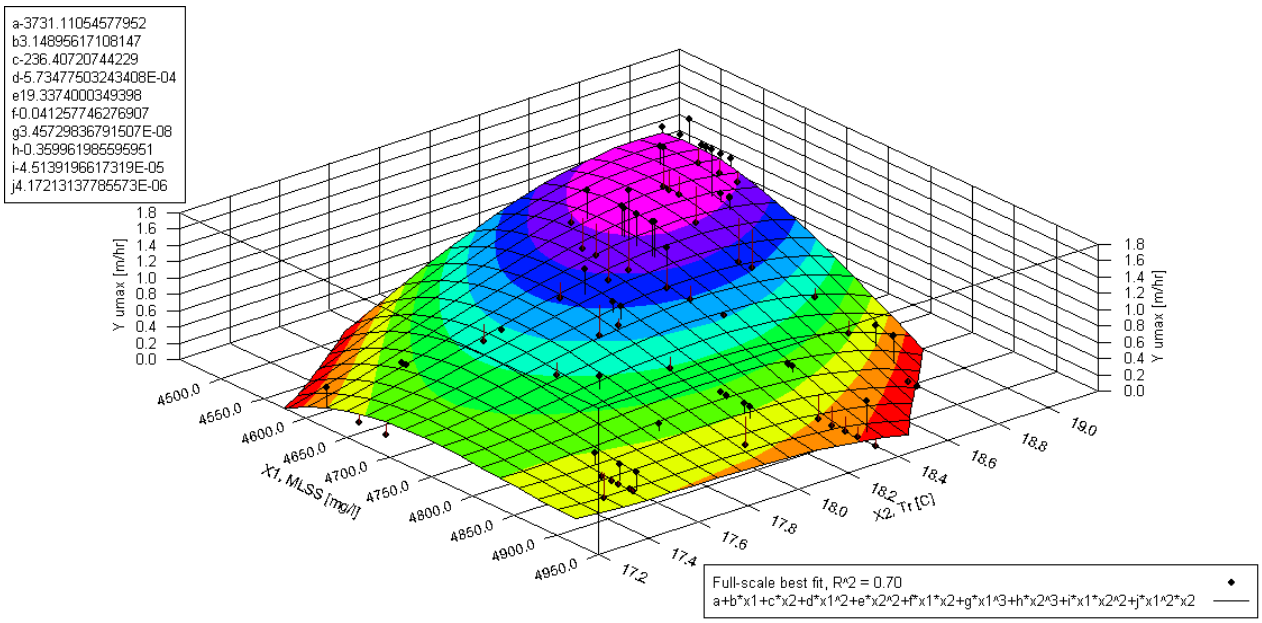

Figure 6-11 u_max related to MLSS concentration and T_r

The temperature impact on MLSS settling is demonstrated by the improved curve fitting when T_r data is included in the full-scale plant u_max evaluation. Figure 6-11 illustrates the relationship between u_max as the response variable, and MLSS concentration and T_r as the dependent variables. The u_max response, after a variation in either or both the MLSS concentration and T_r, can be predicted from Figure 6-11.

The u_max increases from 0 towards 1.7 m/hr, as the MLSS concentration decreases from 4923 to 4489 mg/ℓ, and the T_r increases from 17.2 to 19.0°C. The ideal settling condition of the highest u_max of 1.7 m/hr is obtained at the lowest MLSS concentration and the highest T_r. The inclusion of T_r in u_max correlations improved the curve fitting by a R^2 value of 0.12, from 0.58 to 0.70.

6.3.6 Model fitting: t_umax dependence on MLSS concentration and T_r

The t_umax dependence on MLSS concentration and T_r is statistically evaluated with individual and combined correlations in 2- and 3-D models.

6.3.6.1 t_umax link to MLSS concentration

The recorded data points and a fitted trend for the full-scale on-line MLSS concentration and calculated t_umax are shown in Figure 6-12. The x_1-axis indicates MLSS concentration and the y-axis indicates t_umax. The best-fit curve for t_umax related to MLSS concentration from full-scale data is represented by a polynomial with a R^2 of 0.70, as shown in Figure 6-12.

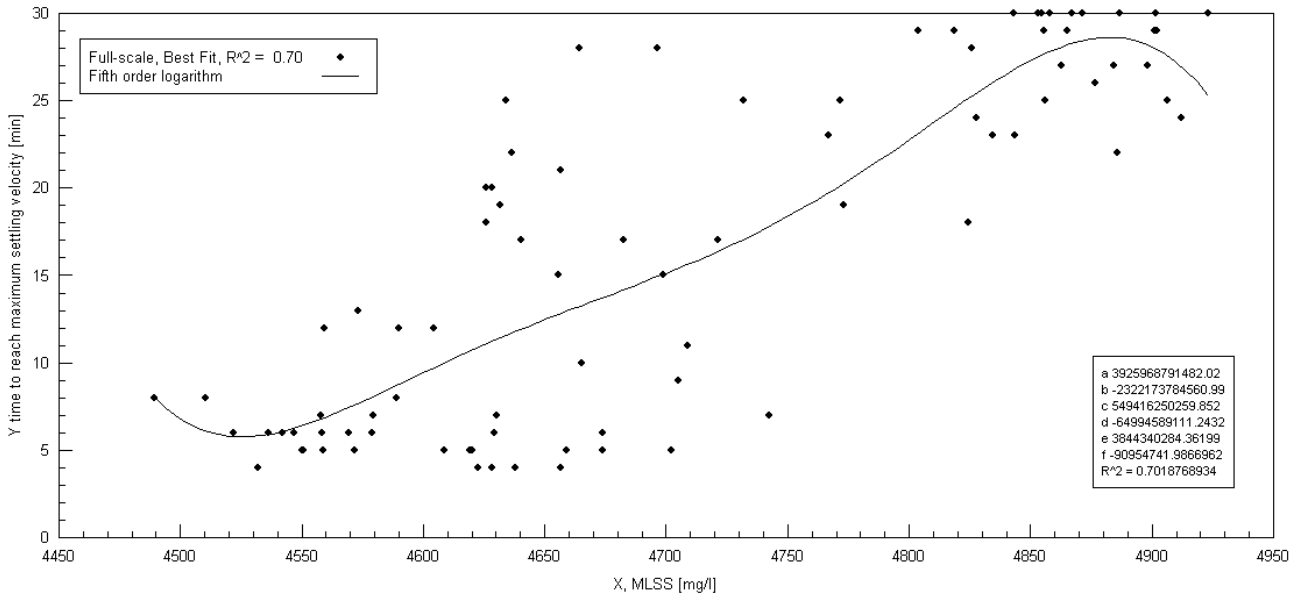

Figure 6-12 t_umax related to MLSS concentration

The direct relationship between t_umax as the response variable and MLSS concentration as the dependent variable is confirmed, since t_umax increases according to the best-fit curve as MLSS concentration increases. The experimental t_umax data scatter is visible from 4 to 30 minutes throughout the MLSS range of 4489 to 4923 mg/ℓ.

6.3.6.2 t_umax link to T_r

The recorded data points and a fitted trend for the on-line T_r and calculated t_umax are shown in Figure 6-13. The x_1-axis indicates T_r and the y-axis indicates t_umax. The best-fit curve for t_umax related to T_r from the full-scale plant data is represented by a polynomial with a very low R^2 of only 0.32.

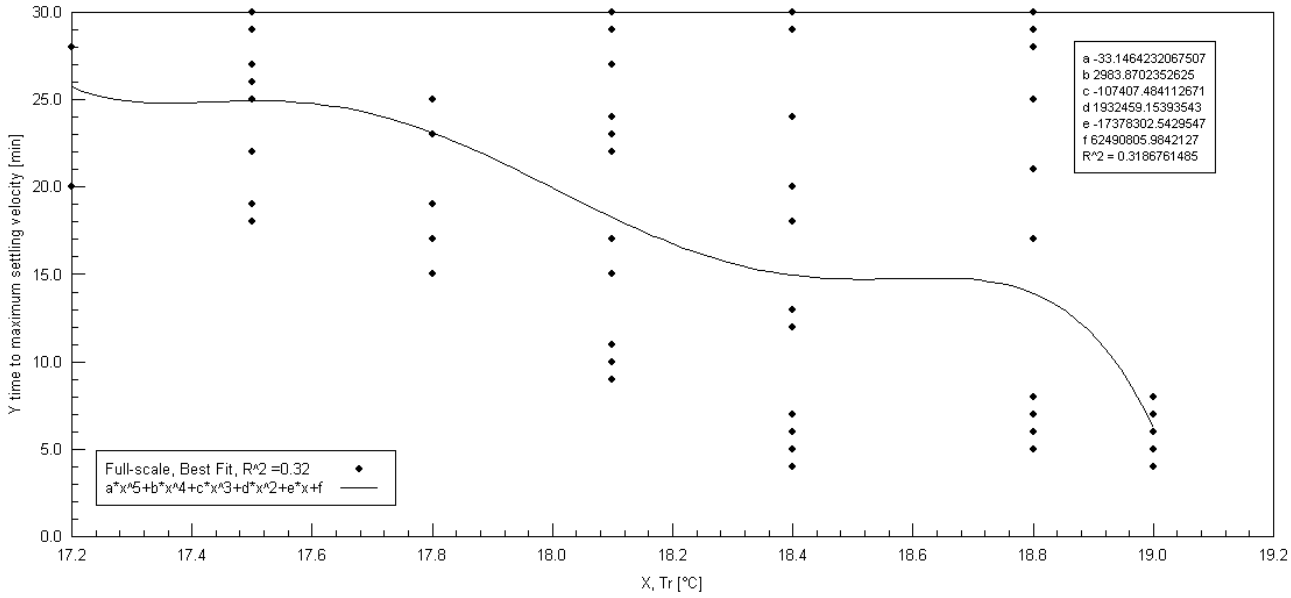

Figure 6-13 t_umax data scatter according to T_r variation

There is a poor correlation visible between t_umax as the response variable and T_r as the dependent variable, as t_umax decreases according to the best-fit curve as T_r increases. The large field of experimental t_umax data scatter was visible throughout the T_r range increments, since the T_r data logger only recorded in 0.3°C increments.

The large data scatter indicates that t_umax data cannot be correlated with only T_r as a single dependent variable. The MLSS concentration is required as a second dependent variable in a 3-D model to reduce the data scatter and to obtain a best-fit correlation for the experimental and calculated data.

6.3.6.3 t_umax link to MLSS concentration and T_r

The recorded data points and fitted correlation for the on-line MLSS concentration, T_r, and calculated t_umax are shown in Figure 6-14. The x_1-, x_2- and y-axis represent MLSS concentration, T_r, and t_umax respectively. The best-fit curve for t_umax related to MLSS concentration and T_r for full-scale plant data was represented on Figure 6-14 by a polynomial with a R^2 of 0.83.

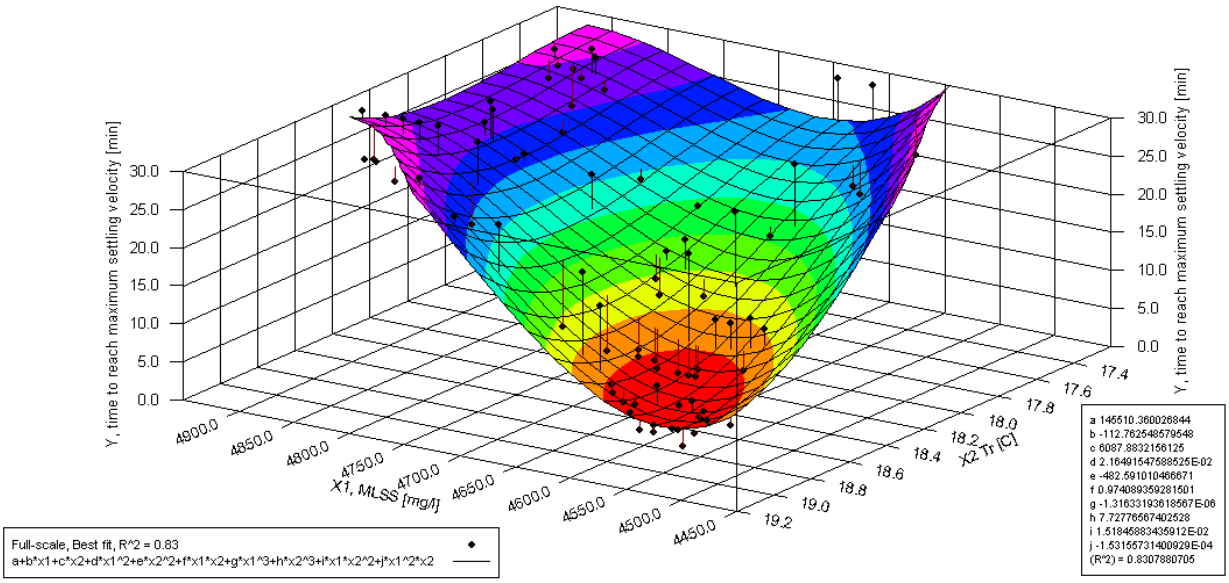

Figure 6-14 t_umax related to MLSS concentration and T_r

The temperature impact on MLSS settling is demonstrated by the improved curve fitting when T_r data is included in the full-scale plant t_umax evaluation. Figure 6-14 illustrates the relationship between t_umax as the response variable, and MLSS concentration and T_r as the dependent variables. The t_umax response, after a variation in either or both the MLSS concentration and T_r, can be predicted from Figure 6-14.

The t_umax increases from 4 towards 30 minutes, as the MLSS concentration increases from 4489 to 4923 mg/ℓ, and the T_r decreases from 19.0 to 17.2°C. The ideal settling condition of the lowest t_umax is obtained at the lowest MLSS concentration and the highest T_r. The inclusion of T_r in t_umax correlations improved the curve fitting by a R^2-value of 0.13, from 0.70 to 0.83.

6.3.7 Model fitting: Summary of curve-fitting correlations

The inclusion of T_r improves the MLSS settling correlations, which is measured according to R^2 increases, as listed in Table 6-2. The average R^2-value for the three MLSS settling parameters (SVI, u_max, t_umax) correlations with MLSS concentration was 0.66 without considering T_r. The inclusion of T_r in the MLSS concentration-based settling correlations improved the average R^2 value by 0.13 to a more acceptable 0.79.

Table 6-2 Best-fit MLSS settling correlations R^2 containing MLSS concentration and T_r

Settling parameter	**MLSS concentration R^2**	**T_r R^2**	**MLSS concentration and T_r R^2**
SVI [mℓ/g]	0.69	0.38	0.84
u_max [m/hr]	0.58	0.26	0.70
t_umax [min]	0.70	0.32	0.83
Average	**0.66**	**0.32**	**0.79**

6.3.8 SVI and settling parameter correlation procedure

SVI-based settling parameter correlations are developed experimentally with the on-line settling meter. These temperature dependent SVI correlations can then be used to predict u_max and t_umax responses over the operational SVI range, as required for plant design or process control purposes.

6.3.8.1 SVI and u_max correlation

The recorded data points and a fitted trend for the full-scale plant calculated SVI and calculated u_max are shown in Figure 6-15. The x_1-axis indicates SVI and the y-axis indicates u_max. The best-fit curve for u_max related to SVI is represented by a polynomial with a R^2 of 0.90.

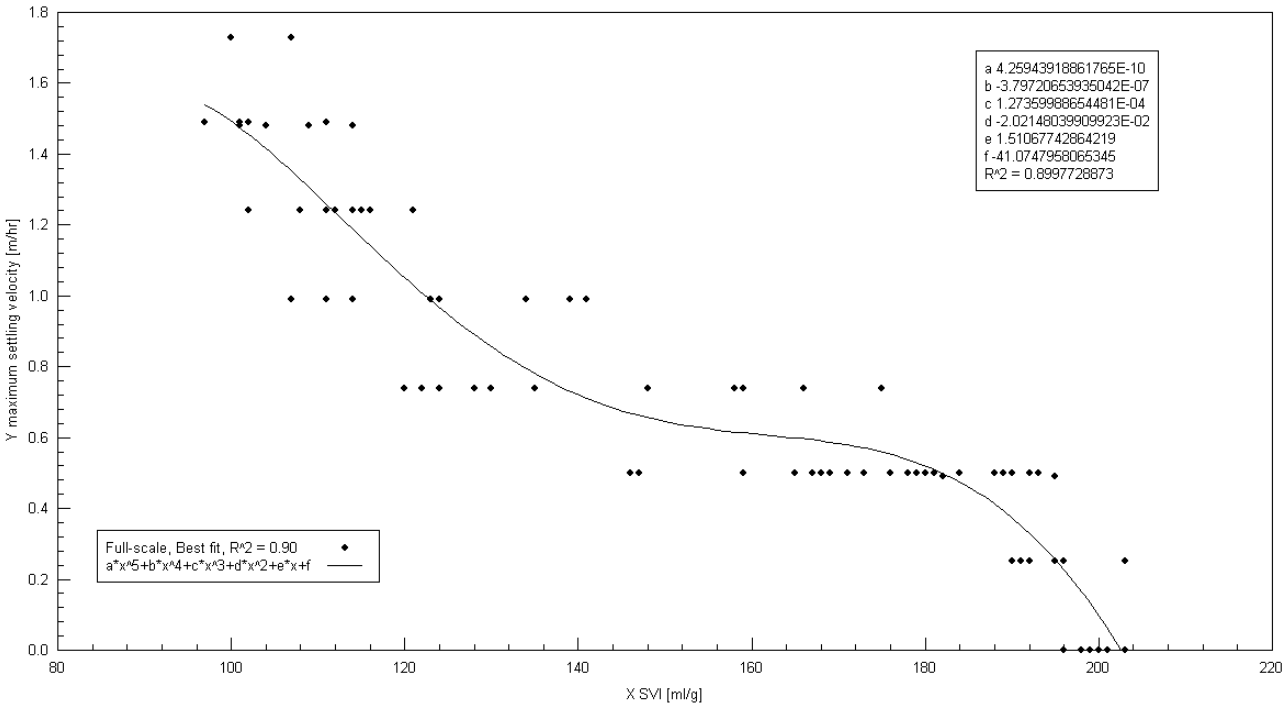

Figure 6-15 u_max related to SVI

The inclusion of T_r in the batch settling tests results in a calculated SVI range from 97 to 203 mℓ/g that correlates in an inverse relationship with u_max from 1.73 to 0 m/hr. The u_max response can now be predicted for a SVI variation, as shown in Figure 6-15. The good correlation between SVI and u_max confirms the results obtained by Sezgin (1982).

6.3.8.2 SVI and t_umax correlation

The recorded data points and a fitted trend for the full-scale plant calculated SVI and calculated t_umax are shown in Figure 6-16. The x_1-axis indicates SVI and the y-axis indicates t_umax. The best-fit curve for t_umax related to SVI is represented by a polynomial with a R^2 of 0.95.

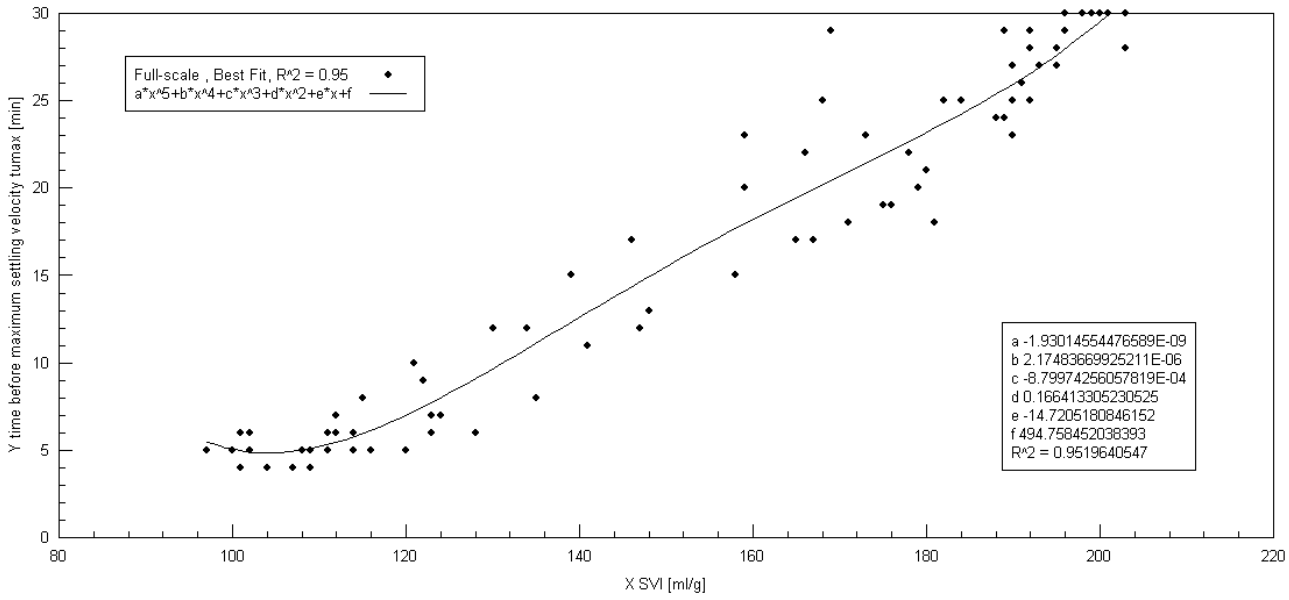

Figure 6-16 t_umax related to SVI

The inclusion of T_r in the batch settling tests results in a calculated SVI range from 97 to 203 mℓ/g that correlates in a direct relationship with t_umax from 4 to 30 minutes. The t_umax response can now be predicted for a SVI variation, as shown in Figure 6-16. Temperature-based settling correlations containing t_umax have not been reported in the available literature.

6.3.9 SVI correlations with u_max and t_umax: Summary of curve-fitting results

SVI data is obtained from on-line automated settling tests that include T_r variation recordings. The calculated SVI correlation with u_max and t_umax is summarised in Table 6-3.

Table 6-3 Summary of SVI correlations with u_max and t_umax

parameter	**R^2**
u_max	0.90
t_umax	0.95
average	**0.93**

The high R^2 of 0.90 and 0.95 illustrate the effect of T_r during MLSS settling. The temperature-based u_max and t_umax correlations with SVI, together with the coefficients, are summarised in Table 6-4.

Table 6-4 Coefficients for polynomial: u_max and t_umax correlations with SVI

coefficient	$y = a * x^5 + b * x^4 + c * x^3 + d * x^2 + e * x + f$, x = SVI [mℓ/g]	
	y = u_max[m/hr]	y = t_umax[minute]
a	4.259E-10	-1.930E-9
b	-3.797E-7	2.175E-6
c	1.274E-4	-8.800E-4
d	-2.021E-2	0.1664
e	1.511	-14.7205
f	-41.075	494.758
R^2	**0.90**	**0.95**

These on-line-based settling parameter correlations with SVI illustrate the benefits of using automatic on-line settling meters. A settling meter detects the MLSS settling profile at T_r. MLSS settling characteristics are plant specific (Wilén, 2006), and on-line-based correlations will therefore reflect the responses of individual plant settling parameters over operational MLSS concentration and T_r ranges.

An on-line MLSS settling meter can be used to predict the settling characteristics of a BNR plant for design and operational purposes:

- a SVI correlation is developed with on-line reactor MLSS concentration and T_r (Figure 6-8),
- the complete SVI range can now be predicted from the known or assumed operational MLSS concentration and T_r ranges (Figure 6-8),
- u_max and t_umax correlations are developed with predicted SVI range (Figure 6-15 and Figure 6-16), and
- the u_max and t_umax range could now be predicted from the calculated SVI range (Figure 6-15 and Figure 6-16).

6.3.10 Simplified settling models: MLSS concentration and T_r

The statistical significance of a model, to account for the fraction of the variation among the data points represented by the model, is illustrated by R^2. Researchers have used R^2 as a general indicator of the statistical significance of settleability models (Daigger, 1995; Ekama *et al.*, 1997), based on batch MLSS settling tests. The following 3-parameter 1st order polynomial function is chosen as the fitted regression model for the 11 settling parameters, based on R^2 and formula simplicity:

$$y = a + \frac{b}{x_1} + \frac{c}{x_2} + \varepsilon, \left(\varepsilon \approx \left(0, \sigma^2\right)\right)$$

where y is the settling parameter, x_1 is the MLSS concentration [mg/ℓ], x_2 is the T_r [°C], a, b, c are regression constants, ε is the random error and σ^2 is the error variance.

This basic model format is easy to use, as summarised in Table 6-5. The 11 equations are a general representation of the experimental data. The data and models are only valid within the experimental MLSS concentration and T_r boundary conditions provided in Table 6-5. Refer also to Table 11-13 in Appendix H for a summary of additional regression variable results. The large t-ratios confirm that all parameters are significant. The low p values indicate that none of the parameters can be removed from the model.

Table 6-5 Summary of regression model constants for settling parameters

Parameter	**4489 mg/ℓ < MLSS concentration < 4923 mg/ℓ, n = 85, ave. = 4705, st. dev. 127** **17.2°C < T_r < 19.0°C, n = 85, ave. = 18.3, st. dev. = 0.5**				
	a	**b**	**c**	**R^2 Simplified**	**R^2 Best-fit**
SVI	872.4200	-4624176.0614	4823.4021	0.71	0.84
t_umax	239.5623	-1290679.9382	939.9347	0.70	0.83
u_max	-9.2997	57454.2585	-39.8603	0.59	0.70
u_ave	-2.8943	18433.8191	-15.1792	0.76	0.87
h	1793.9619	-9200670.3014	7744.0213	0.76	0.87
u1	-1.1851	14418.7348	-31.9946	0.32	0.45
u2	-2.6708	33145.3653	-74.7660	0.59	0.71
u3	-3.6732	25152.0675	-26.7192	0.62	0.79
u4	-4.1828	19564.9547	3.4218	0.60	0.79
u5	-3.3897	11822.7573	18.7500	0.34	0.56
u6	-2.6835	8411.5793	18.8984	0.30	0.50

6.3.10.1 SVI correlation with MLSS concentration and T_r

The response relationship of SVI to MLSS concentration and T_r variations, obtained from the full-scale plant data, is presented by the following regression model, with $R^2 = 0.71$:

$$SVI = 872.4 - \frac{4624176.1}{MLSS} + \frac{4823.4}{T_r} \quad [m\ell/g] \qquad \text{Equation 6-1}$$

The plot of this model is shown in Figure 6-17. The x_1-axis represents the MLSS concentration range of 4489 to 4923 mg/ℓ, the x_2-axis represents the T_r range from 17.2 to 19.0°C, and the y_1-axis represents the SVI from 96 mℓ/g to 214 mℓ/g. The model is represented by a best-fit polynomial with a $R^2 = 0.84$.

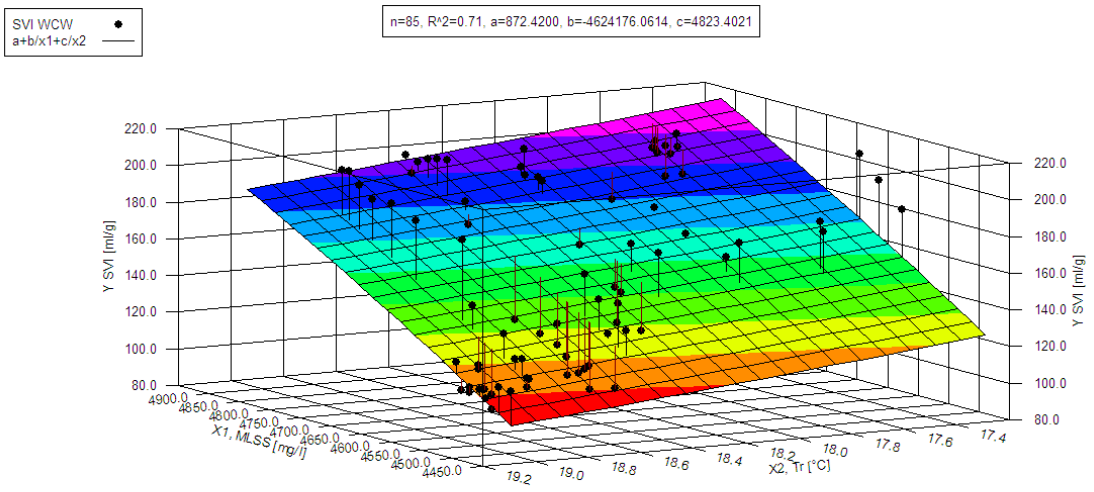

Figure 6-17 SVI dependency on MLSS concentration and T_r

The SVI dependence on the full-scale T_r can be illustrated with a simulation. At an average constant MLSS concentration of 4500 mg/ℓ, the SVI change due to a T_r reduction from 19.0 to 17.2°C can be determined according to the SVI-model (Equation 6.1). The SVI increases by 26.5 mℓ/g, from 98.7 to 125.2 mℓ/g, with a corresponding relative SVI increase of 14.8 mℓ/g SVI per 1°C T_r reduction, or -14.8 mℓ/g SVI/1°C T_r.

This SVI correlation illustrates the extent of batch MLSS settling test result variations. The relatively small temperature reduction of 1.8°C contributes to a SVI increase of 26.5 mℓ/g. MLSS samples are taken from a reactor at T_r, and they are usually transported, stored, and tested at a different T_s, which could change by much more than 1.8°C.

6.3.10.2 u_max correlation with MLSS concentration and T_r

The response relationship of u_max to MLSS concentration and T_r variations is presented by the following regression model, with $R^2 = 0.59$:

$$u\_max = -2.2 + \frac{14785.4}{MLSS} - \frac{8.3}{T_r} \ [m/hr] \qquad \text{Equation 6-2}$$

The plot of this model is shown in Figure 6-18. The x_1-axis represents the MLSS concentration range of 4489 to 4923 mg/ℓ, the x_2-axis represents the T_r range from 17.2 to 19.0°C, and the y-axis represents the u_max from 0.1 to 1.4 m/hr. The model is represented by a best-fit polynomial with $R^2 = 0.70$.

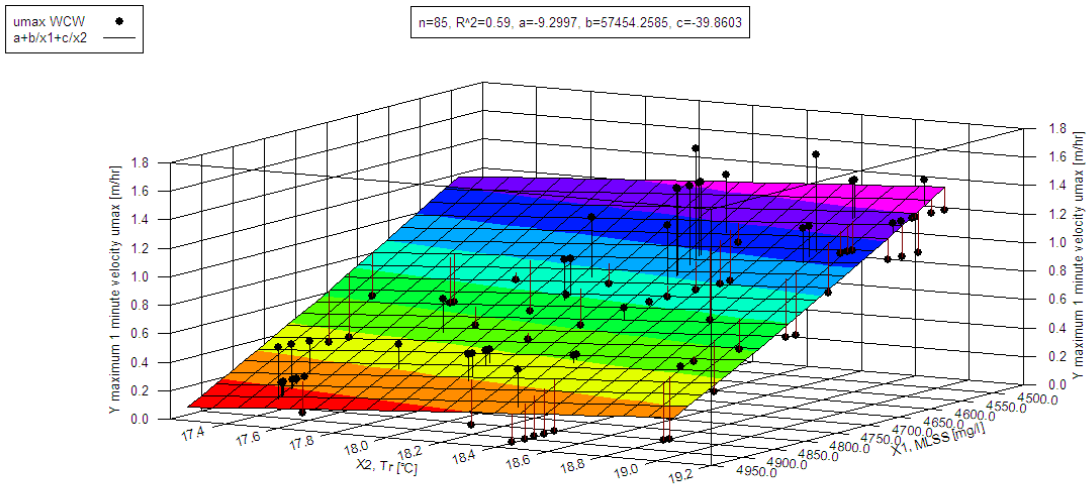

Figure 6-18 u_max dependency on MLSS concentration and T_r

A simulation can illustrate the dependence of u_max on the operational T_r. At an average constant MLSS concentration of 4500 mg/ℓ, the u_max change due to a T_r reduction from 19.0 to 17.2°C can be determined according to the u_max-model (Equation 6.2). The u_max decreases by 0.2 m/hr, from 1.4 to 1.2 m/hr, with a corresponding relative u_max decrease of 0.1 m/hr per 1°C T_r reduction, or 0.1m/hr u_max/1°C T_r.

These correlations have implications for full-scale MLSS settling control. The typical diurnal T_r variation of 1.8°C at a constant MLSS concentration, contributes to an u_max change of more than 0.1 m/hr. From the relatively low T_r dependence of u_max, it might

be argued that the 1-minute interval in the MLSS settling meter is not sensitive enough to reflect the true zone settling velocity. An improved u_max recording process is required for the on-line settling meter. It is recommended that the MLSS settling meter recording time interval be changed in future applications from 1 to at least 0.5 minutes.

These u_max settling velocity correlations have implications for clarifier design. Secondary tank clarifier design is usually conservative and based on bad MLSS settling characteristics (Van Haandel, 1992). The lower u_max will require a larger secondary settling tank capacity to ensure the solids load can be accommodated at the higher MLSS concentration and the lower T_r.

6.3.10.3 t_umax correlation with MLSS concentration and T_r

The response relationship of t_umax to MLSS concentration and T_r variations is presented by the following regression model, with R^2= 0.70:

$$t\_u\max = 239.6 - \frac{1290679.9}{MLSS} + \frac{939.9}{T_r} \ [\text{minute}] \qquad \text{Equation 6-3}$$

The plot of this model is shown in Figure 6-19. The x_1-axis represents the MLSS concentration range of 4489 to 4923 mg/ℓ, the x_2-axis represents the T_r range from 17.2 to 19.0°C, and the y-axis represents the t_umax from 2 to 30 minutes. This model is represented by a best-fit polynomial with a R^2 = 0.83.

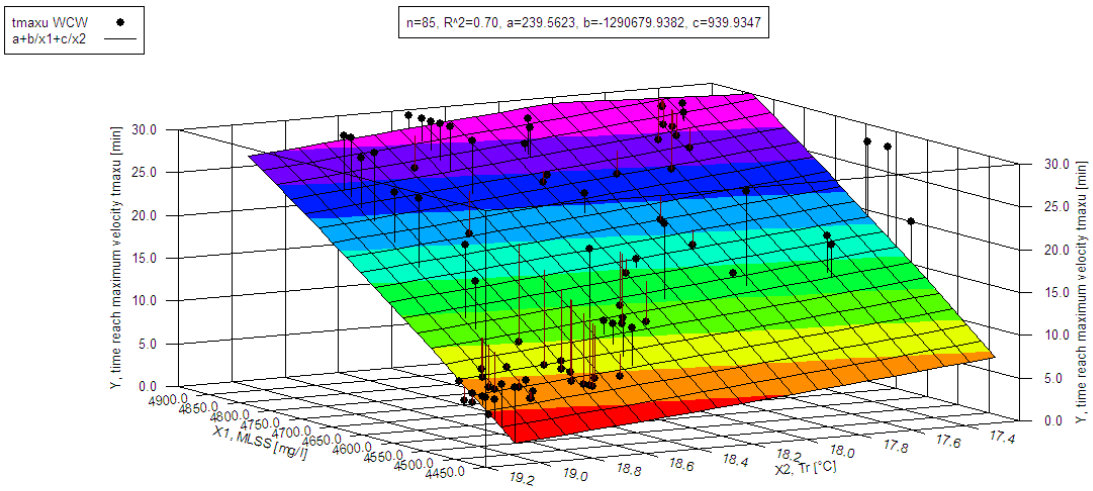

Figure 6-19 t_umax dependency on MLSS concentration and T_r

A simulation can illustrate the dependence of t_umax on T_r. At an average constant MLSS concentration of 4500 mg/ℓ, the t_umax change due to a T_r reduction from 19.0 to 17.2°C can be determined according to the t_umax-model (Equation 6.3). The t_umax increases by 4.2 minutes, from 2.2 to 6.5 minutes, with a corresponding relative t_umax increase of 2.4 minutes per 1°C T_r reduction, or 2.4 minute t_umax/1°C T_r.

These correlations have implications for MLSS settling control and design. The typical diurnal reactor temperature variation of 1.8°C, at a constant MLSS concentration, contributes to a reflocculation time increasing from 2.2 to 6.5 minutes (when u_max commences). The reflocculation lag time delay will require a larger stilling chamber to ensure reflocculation will take place at higher MLSS concentrations and T_r.

The correlations also have implications for MLSS sample handling. The dilution of the MLSS concentration of a sample for a DSVI calculation reduces the t_umax, as the bioflocs can start settling immediately as discrete particles. Sample handling, transport, storage, and tests at different room temperatures can lead to large temperature variations, as well as a corresponding change in reflocculation time.

6.3.10.4 u_ave correlation with MLSS concentration and T_r variation

The response relationship of u_ave to MLSS concentration and T_r variations is presented by the following regression model, with R^2= 0.76:

$$u\_ave = -2.9 + \frac{18433.8}{MLSS} - \frac{15.2}{T_r} \text{ [m/hr]} \qquad \text{Equation 6-4}$$

The plot of this model is presented in Figure 6-20. The x_1-axis represents the MLSS concentration range of 4489 to 4923 mg/ℓ, the x_2-axis represents the T_r range from 17.2 to 19.0°C, and the y-axis represents u_ave from 0 to 0.4 m/hr. This model is represented by a best-fit polynomial with a R^2 = 0.87.

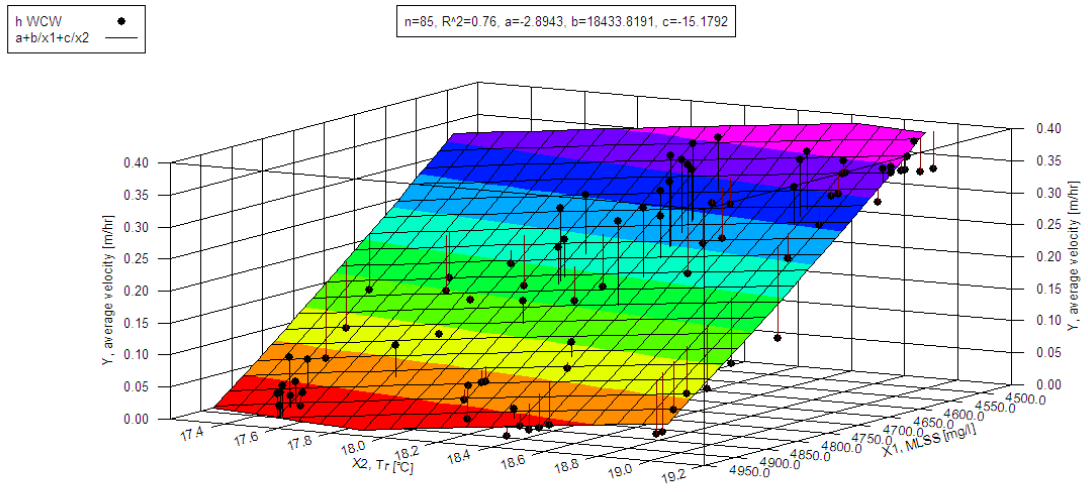

Figure 6-20 u_ave dependency on MLSS concentration and T_r

A simulation can illustrate the dependence of u_ave on the T_r. At an average constant MLSS concentration of 4500 mg/ℓ, the u_ave change due to a T_r reduction from 19.0 to 17.2°C can be determined according to the u_ave-model (Equation 6.4). The u_ave decreases by 0.1 m/hr, from 0.4 to 0.3 m/hr, with a corresponding relative u_ave decrease of 0.04 m/hr per 1°C T_r reduction, or 0.04 m/hr u_ave/ 1°C T_r.

The u_ave over 30 minutes is a rapid indicator of MLSS settling velocity, with the advantage that it can be directly calculated from the SV_{30} (according to MLSS height h settled over 30 minutes). The u_ave, as a general settling index, has similar shortcomings to the SVI, specifically regarding the height of the test cylinder or column used. It does not give any indications of MLSS settling changes occurring during the settling period. The parameter u_ave should be used with caution as a general settling indicator. For this study, the principle aim was to demonstrate the T_r dependence of u_ave, as shown in Figure 6-20.

6.3.10.5 h correlation with MLSS concentration and T_r variation

The response relationship of h to MLSS concentration and T_r variations obtained from the full-scale plant data is presented by the following regression model, with R^2= 0.76:

$$h = 1794.0 - \frac{9200670.3}{MLSS} - \frac{7744.0}{T_r} \text{ [mm]} \qquad \text{Equation 6-5}$$

The plot of this model is presented in Figure 6-21. The x_1-axis represents the MLSS concentration range of 4489 to 4923 mg/ℓ, the x_2-axis represents the T_r range from 17.2 to 19.0°C, and the y-axis represents h from 152 to 355.9 mm. This model is represented by a best-fit polynomial with a $R^2 = 0.87$.

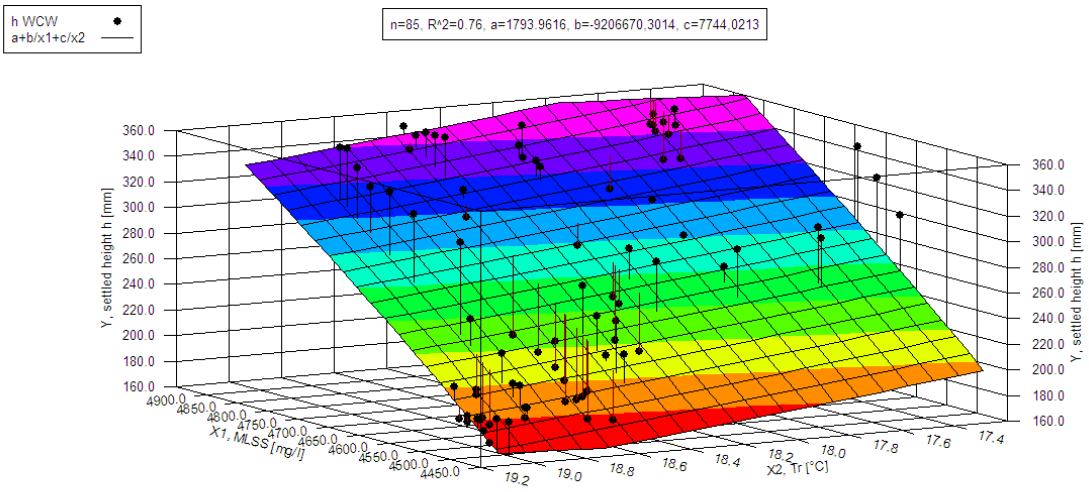

Figure 6-21 h dependency on MLSS concentration and T_r

A simulation can illustrate the dependence of h on T_r. At an average constant MLSS concentration of 4500 mg/ℓ, the h change due to a T_r reduction from 19.0 to 17.2°C can be determined according to the h-model (Equation 6.5). The h increases by 35 mm, from 157 to 192 mm, with a corresponding relative h increase of 19 mm per 1°C T_r reduction, or -19 mm h /1°C T_r.

6.3.10.6 Incremental velocity u1 to u6 simulation over 30 minutes

The 30-minute settling period is divided in 6 settling periods of 5 minutes each. The average settling velocity over these 5-minute periods is calculated as u1, u2, u3, u4, u5, u6. It was previously demonstrated that MLSS samples will settle faster and sooner (u_max higher and t_umax lower) at lower MLSS concentrations and at higher T_r.

For MLSS samples at a low MLSS concentration and a high T_r, the t_umax will be low and u1, u2, and u3 will therefore be higher. For MLSS samples at a high MLSS concentration and a low T_r, the t_umax will be higher. These MLSS samples will only

settle later in the 30-minute cycle, and u4, u5, and u6 will be subsequently higher for these unfavourable MLSS settling conditions (high MLSS concentration and low T_r).

To illustrate the incremental settling velocity changes according to MLSS concentration and T_r, the following 6 sections provide simplified models and regression graphs for u1 to u6.

6.3.10.7 u1 correlation with MLSS concentration and T_r variation

The response relationship of u1 (0 to 5 minutes) to MLSS concentration and T_r variations is presented by the following equation:

$$u1 = -1.2 + \frac{14418.7}{MLSS} - \frac{32.0}{T_r} \quad [m/hr] \qquad \text{Equation 6-6}$$

The model plot is shown in Figure 6-22, and u1 varies on the y-axis from 0 to 0.34 m/hr.

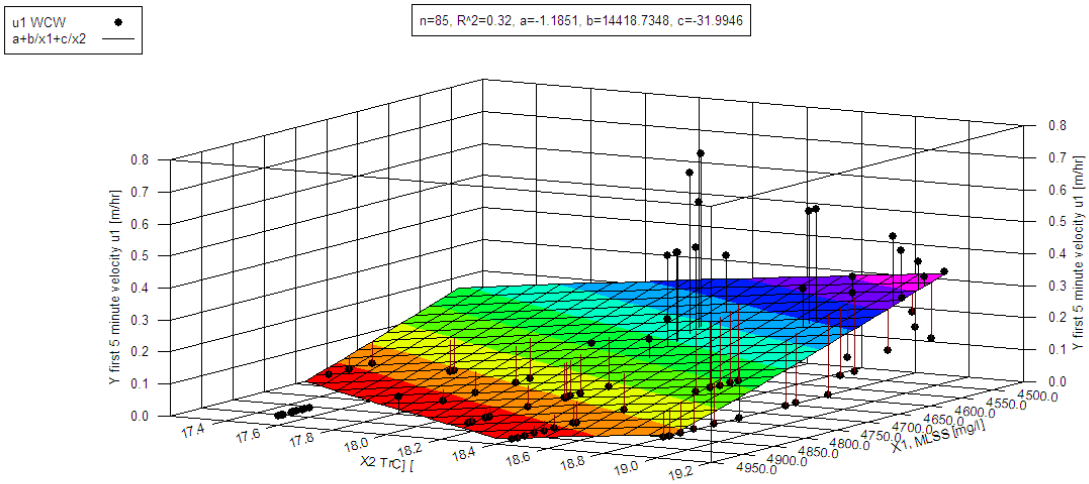

Figure 6-22 u1 dependency on MLSS concentration and T_r

A simulation can illustrate the dependence of the u1 on T_r. At an average constant MLSS concentration of 4500 mg/ℓ, the u1 change due to a T_r reduction from 19.0 to 17.2°C can be determined according to the u1-model (Equation 6.6). The u1 reduces from 0.34 to 0.19 m/hr, with a corresponding relative u1 decrease of 0.08 m/hr per 1°C T_r reduction, or 0.08 m/hr u1/1°C T_r.

The correlation between u1 and MLSS concentration is not represented in traditional models. The direct correlation between u1 and T_r is now illustrated with on-line evaluations, at an average of 0.08 m/hr per 1°C change. The correlations can be used as an indication of the reflocculation time. An u1 settling velocity of 0 m/hr indicates that the MLSS is still in suspension after 5 minutes and stage 2 zone settling has not started. The inverse correlation between t_umax and T_r is now illustrated for on-line evaluations according to the MLSS settling velocity.

These correlations can be used together with the reflocculation time to aid in the design of stilling chamber capacity, to ensure bioflocculation will take place at higher MLSS concentrations and lower T_r. The ISV will determine the loading capacity of the secondary settling tank (Wilén *et al.*, 2006).

6.3.10.8 u2 correlation with MLSS concentration and T_r variation

The response relationship of u2 (5 to 10 minutes) to MLSS concentration and T_r variations is presented by the following equation:

$$u2 = -2.7 + \frac{33145}{MLSS} - \frac{74.8}{T_r} \quad [m/hr] \qquad \text{Equation 6-7}$$

The model plot is shown in Figure 6-23 , and u2 varies on the y-axis from 0 to 0.78 m/hr.

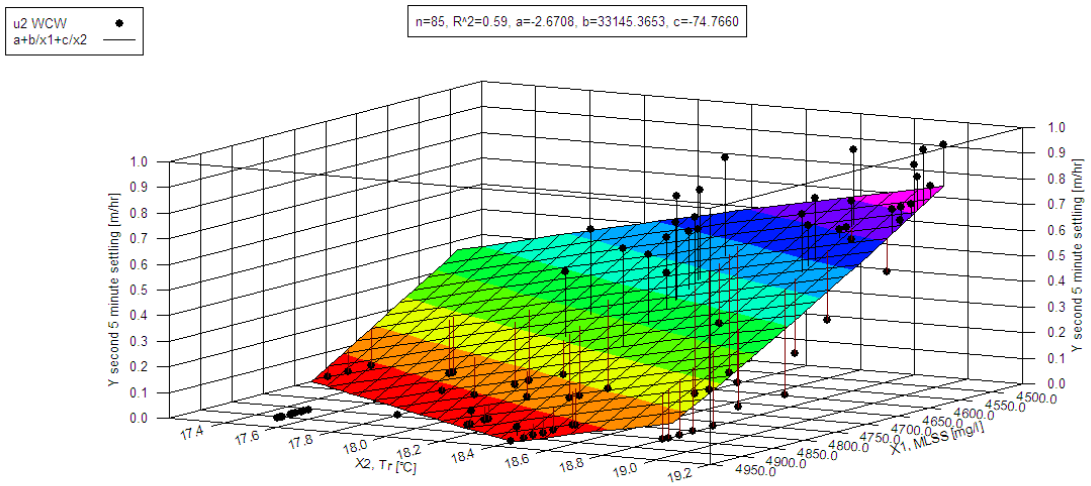

Figure 6-23 u2 dependency on MLSS concentration and T_r

A simulation can illustrate the dependence of the u2 on T_r. At an average constant MLSS concentration of 4500 mg/ℓ, the u2 change due to a T_r reduction from 19.0 to 17.2°C can be determined according to the u2-model (Equation 6.7). The u2 reduces from 0.76 to 0.42 m/hr, with a corresponding relative u2 decrease of 0.19 m/hr per 1°C T_r reduction, or 0.19 m/hr u1/1°C T_r.

The correlation between u2 and MLSS concentration is not represented in traditional models. The direct correlation between u2 and T_r is illustrated with on-line evaluations, at an average of 0.19 m/hr per 1°C change. The correlation can be used, together with u1, as an indication of the reflocculation time. An u2 settling velocity of 0 m/hr indicates that the MLSS is in suspension after 10 minutes and zone settling has not started. The inverse correlation between time to reach maximum settling velocity and T_r is now illustrated with on-line evaluations. These correlations can be used together with the reflocculation time to aid with design of stilling chamber capacity, to ensure bio-flocculation will take place in stilling chambers at higher MLSS concentrations and lower T_r.

6.3.10.9 u3 correlation with MLSS concentration and T_r variation

The response relationship of u3 (10 to 15 minutes) to MLSS concentration and T_r variations is presented by the following equation:

$$u3 = -3.7 + \frac{25152.1}{MLSS} - \frac{26.7}{T_r} \quad [m/hr] \qquad \text{Equation 6-8}$$

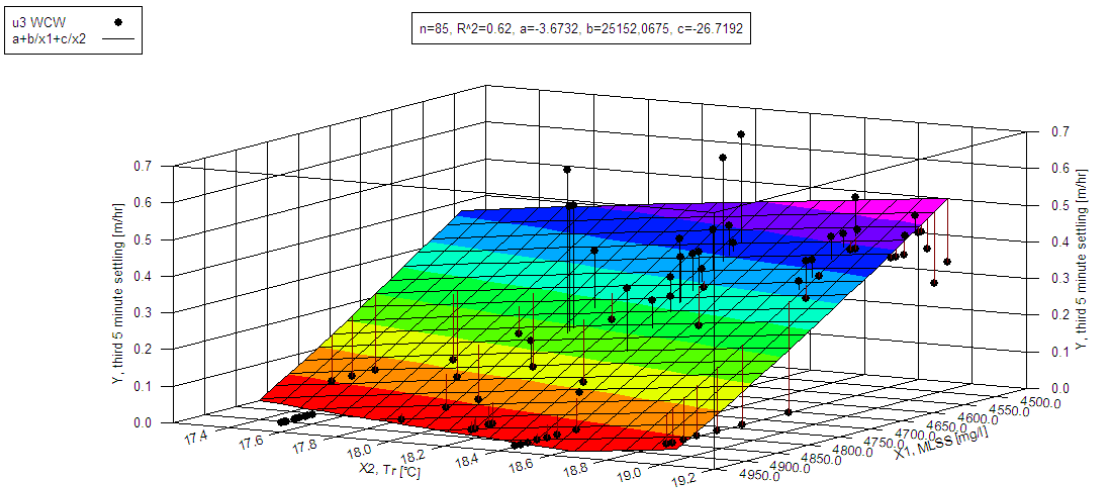

Figure 6-24 u3 dependency on MLSS concentration and T_r

The model plot is shown in Figure 6-24, and u3 varies on the y-axis from 0 to 0.52 m/hr.

A simulation can illustrate the dependence of the u3 on T_r. At an average constant MLSS concentration of 4500 mg/ℓ, the u3 change due to a T_r reduction from 19.0 to 17.2°C can be determined according to the u3-model (Equation 6.8). The u3 reduces from 0.51 to 0.39 m/hr, with a corresponding relative u3 decrease of 0.07 m/hr per 1°C T_r reduction, or 0.07 m/hr u3/1°C T_r.

The correlation between u3 and MLSS concentration is not represented in traditional models. The direct correlation between u3 and T_r is now illustrated for on-line evaluations, at an average of 0.07 m/hr per 1°C change. The colder MLSS samples at higher MLSS concentrations only start to settle after 10 minutes, and the u3 incremental settling velocity is therefore higher at the high MLSS concentration and the low T_r range.

6.3.10.10 u4 correlation with MLSS concentration and T_r variation

The response relationship of u4 (15 to 20 minutes) to MLSS concentration and T_r variations is presented by the following equation:

$$u4 = -4.2 + \frac{19565.0}{MLSS} + \frac{3.4}{T_r} \quad [m/hr] \qquad \text{Equation 6-9}$$

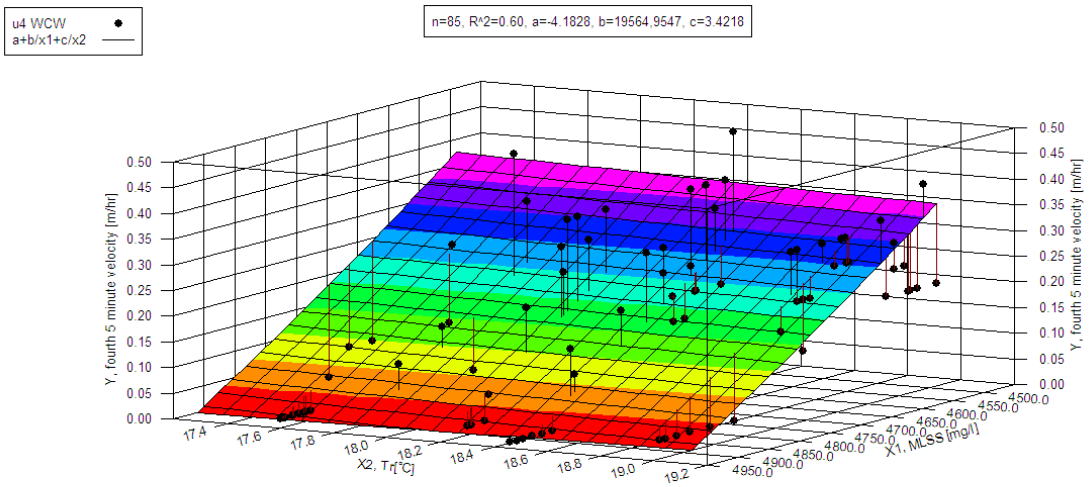

Figure 6-25 u4 dependency on MLSS concentration and T_r

The model plot is shown in Figure 6-25, and u4 varies on the y-axis from 0 to 0.37 m/hr.

A simulation can illustrate the dependence of the u4 on T_r. At an average constant MLSS concentration of 4500 mg/ℓ, the u4 change due to a T_r reduction from 19.0 to 17.2°C can be determined according to the u4-model (Equation 6.9). The u4 increases from 0.35 to 0.36 m/hr, with a corresponding relative u4 increase of 0.01 m/hr per 1°C T_r reduction, or - 0.01 m/hr u4/1°C T_r.

The correlation between u4 and MLSS concentration is not represented in traditional models. The u4 (settling velocity over the fourth 5-minute settling period) follows now a different pattern from previous incremental velocities up to 15 minutes. All the easily flocculating MLSS at the high temperature has flocculated and settled over these first 15 minutes. The MLSS at the colder temperature only starts to settle after 15 minutes, and u4 is therefore higher in the low temperature range. The inverse correlation between u4 and T_r is illustrated from the on-line evaluations at an average of -0.01 m/hr per 1°C change.

6.3.10.11 u5 correlation with MLSS concentration and T_r variation

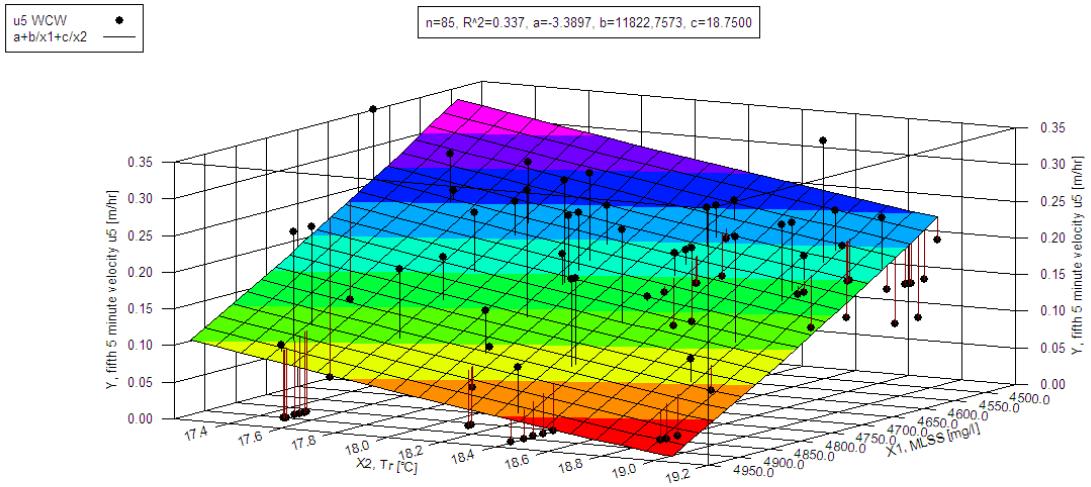

Figure 6-26 u5 dependency on MLSS concentration and T_r

The response relationship of u5 (20 to 25 minutes) to MLSS concentration and T_r variations is presented by the following equation:

$$u5 = -3.4 + \frac{11822.8}{MLSS} + \frac{18.8}{T_r} \quad [m/hr] \qquad \text{Equation 6-10}$$

The model plot is shown in Figure 6-26, and u5 varies on the y-axis from 0 to 0.33 m/hr.

A simulation can illustrate the dependence of the u5 on T_r. At an average constant MLSS concentration of 4500 mg/ℓ, the u5 change due to a T_r reduction from 19.0 to 17.2°C can be determined according to the u5-model (Equation 6.10). The u5 increases from 0.22 to 0.31 m/hr, with a corresponding relative u5 increase of 0.05 m/hr per 1°C T_r reduction, or - 0.05 m/hr u5/1°C T_r.

The correlation between u5 and MLSS concentration is not represented in traditional models. The settling velocity over the fifth 5-minute settling period now follows the same inverse pattern as identified previously in u4. All the easily flocculating MLSS at the high temperature has flocculated and settled over the first 15 minutes. Some MLSS sample at the colder temperature only start to settle after 20 to 25 minutes, and the settling velocity is therefore higher in the lower temperature range. The inverse correlation between u5 and T_r is illustrated for on-line evaluations at an average of -0.05 m/hr per 1°C change.

6.3.10.12 u6 correlation with MLSS concentration and T_r variation

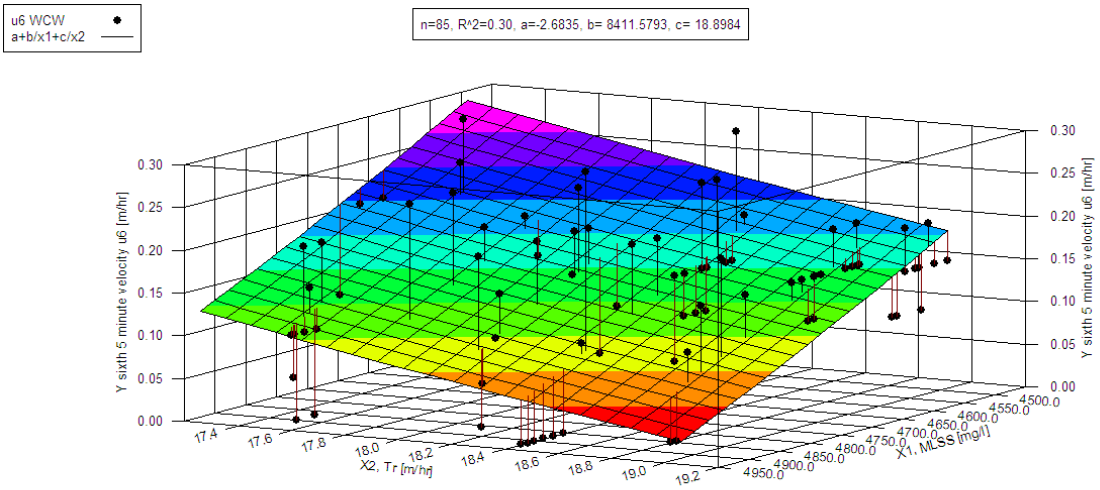

Figure 6-27 u6 dependency on MLSS concentration and T_r

The response relationship of u6 (25 to 30 minutes) to MLSS concentration and T_r variations is presented by the following equation:

$$u6 = -2.7 + \frac{8411.6}{MLSS} + \frac{18.9}{T_r} \quad [m/hr] \qquad \text{Equation 6-11}$$

The model plot is shown in Figure 6-27, and u6 varies on the y-axis from 0.02 to 0.29 m/hr.

A simulation can illustrate the dependence of u6 on T_r. At an average constant MLSS concentration of 4500 mg/ℓ, the u6 change due to a T_r reduction from 19.0 to 17.2°C can be determined according to the u6-model (Equation 6.11). The u6 increases from 0.18 to 0.27 m/hr, with a corresponding relative u6 increase of 0.05 m/hr per 1°C T_r reduction, or - 0.05 m/hr u6/1°C T_r.

The settling velocity over the sixth 5-minute period now follows the same pattern as identified in u4 and u5. All the easily flocculating MLSS at higher temperatures has flocculated and settled over the first 15 minutes. The MLSS at the colder temperature only starts to settle after 15 to 25 minutes, and the u6 settling velocity is therefore higher in the lower T_r range. The inverse correlation between u6 and T_r is illustrated for the on-line evaluation, at an average of -0.05 m/hr per 1°C change.

6.3.11 Settling models results summary

The experimental range for settling parameters is provided in Table 6-6. Modelled values differ slightly from experimental values due to regression curve-fitting calculations.

Table 6-6 Settling parameters model prediction over experimental range

Parameter	Unit	Minimum experimental parameter value	Minimum modelled parameter value	Maximum experimental parameter value	Maximum modelled parameter value
SVI	[mℓ/g]	97	96.2	203	213.5
t_umax	[min.]	4.0	1.5	30.0	32.0
u_max	[m/hr]	0.00	0.05	1.73	1.40
u_ave	[m/hr]	0.01	-0.03	0.39	0.41
h	[mm]	162.0	151.9	355.9	375.3
u1	[m/hr]	0.00	-0.12	0.74	0.34
u2	[m/hr]	0.00	-0.28	0.94	0.78
u3	[m/hr]	0.00	-0.12	0.69	0.52
u4	[m/hr]	0.00	-0.03	0.49	0.37
u5	[m/hr]	0.00	0.00	0.35	0.33
u6	[m/hr]	0.00	0.02	0.30	0.29

The experimental parameter list is compared to the modelled range for the same parameters, with the minimum and maximum values indicating the comparative predicted values. The model equation can be recalculated with a new parameter range, if the predicted values fall outside the experimental range.

Model equations were not recalculated, as the principle aim of the modelling was to illustrate T_r-based MLSS settling correlations for a full-scale plant-specific experimental condition. The development of more representative parameter models will require additional experimental data over a wider operational range.

6.3.12 Settling models simulation results

An average MLSS concentration of 4500 mg/ℓ is used with the boundary temperature range from 19.0 to 17.2°C to calculate settling parameters. The results are summarised in Table 6-7. The relative change to settling parameters is based on a 1°C T_r reduction. Direct and inverse relationships are quantified respectively by positive and negative parameter changes.

Table 6-7 Modelled settling parameters simulation based on T_r variation

Parameter	MLSS concentration constant [mg/ℓ]	Tr High [°C]	calculated parameter	Tr Low [°C]	Tr change [°C]	calculated parameter	parameter change	parameter relative change	unit
SVI	4500	19.0	99	17.2	1.8	125	-26.5	-14.8	mℓ/g/1°C
t_umax	4500	19.0	2.2	17.2	1.8	6.5	-4.2	-2.4	min/1°C
u_max	4500	19.0	1.4	17.2	1.8	1.2	0.2	0.1	m/hr/1°C
u_ave	4500	19.0	0.4	17.2	1.8	0.3	0.1	0.04	m/hr/1°C
h	4500	19.0	157	17.2	1.8	192	-35	-19	mm/1°C
U1	4500	19.0	0.34	17.2	1.8	0.19	0.14	0.08	m/hr/1°C
U2	4500	19.0	0.76	17.2	1.8	0.42	0.34	0.19	m/hr/1°C
U3	4500	19.0	0.51	17.2	1.8	0.39	0.12	0.07	m/hr/1°C
U4	4500	19.0	0.35	17.2	1.8	0.36	-0.02	-0.01	m/hr/1°C
U5	4500	19.0	0.22	17.2	1.8	0.31	-0.08	-0.05	m/hr/1°C
U6	4500	19.0	0.18	17.2	1.8	0.27	-0.09	-0.05	m/hr/1°C

6.4 Summary

A custom-made automated MLSS settling meter provides semi-continuous MLSS settling profiles for use in settling parameter modelling. The experimental work consists of four main aspects at a full-scale plant reactor:

1. diurnal variations in h, T_r, MLSS concentration, and SVI,
2. best-fit modelling of three settling parameters (SVI, u_max and t_umax) with MLSS concentration and T_r,
3. model fitting of SVI with u_max and t_umax, and
4. basic modelling and simulation of 11 settling parameters with MLSS concentration and T_r.

The on-line MLSS settling evaluation at a full-scale plant reactor provides the following results:

- The diurnal trends follow sinusoidal wave profiles, with an inverse relationship between T_r and settling meter h, MLSS concentration, and SVI,

- The SVI, u_max, and t_umax were unsatisfactorily correlated to MLSS concentration alone, with R^2-values of 0.69, 0.58, and 0.70 respectively due to visible data scatter. The inclusion of T_r improved the corresponding best-fit correlations to R^2-values of 0.84, 0.70, and 0.83, with large t-ratios and low p values indicating the importance of T_r,

- The temperature-based SVI was correlated to u_max and t_umax at R^2-values of 0.90 and 0.95 respectively,

- The basic 3-parameter settling model provided significant changes for the 11 settling parameter, based on simulated operational T_r variations at constant MLSS concentrations, as summarised in Table 6-7.

6.5 Conclusions

- The governing role of MLSS concentration during MLSS settling might hide the effects of other factors affecting MLSS settling, such as temperature. The settling parameters, such as SVI, mirror the diurnal MLSS concentration profile, but the diurnal temperature fluctuation changes inversely with the corresponding MLSS concentration. The on-line MLSS settling meter collects enough data points based on operational conditions to generate temperature dependent MLSS settling profiles that identify and represent the effects of temperature.

- The small, but significant effect of short-term temperature variation on MLSS settling is proved statistically with improved settling models. Settling parameters are unsatisfactorily correlated with MLSS concentration alone. The inclusion of T_r improved the corresponding best-fit correlations, with R^2-values increases larger than 0.1 obtained for the full-scale plant data.

- The temperature effect on settling parameters is illustrated with simplified settling models. Simulations illustrate the changes to settling parameters, based on temperature changes at constant MLSS concentrations. The SVI increase of 14.8 mℓ/g per 1°C T_r reduction is coincidentally identical to the batch settling SVI test results (-14.8 mℓ/g per 1°C T_s). The time to reach u_max increases by 2.4 minutes per 1°C T_r reduction, while the u_max increases by 0.1 m/hr per 1°C T_r increase.

- The incremental 5-minute settling velocity models produce distinctive trends over the 30-minute settling period:

1. A direct relationship exists over the first 15 minutes between u1, u2, u3, and T_r, similar to the u_ave and u_max relationships with T_r,
2. After 15 minutes, the settling trend changes, and for the next 15 minutes u4, u5, and u6 change inversely with T_r variations, and
3. MLSS samples at higher MLSS concentration and lower T_r did not settle over the first 15 minutes, and the colder MLSS samples only started to settle between 15 and 30 minutes, creating inverse MLSS settling velocity to T_r relationships.

- The modelled settling parameter values are only valid for the experimental boundary conditions, as indicated on the individual graphs. Predictions based on the settling parameter models are invalid outside these tested MLSS concentration and T_r ranges.

- With the above conclusions, a suitable approach is provided to improve the reliability of MLSS settling tests. The effects of short-term temperature variations before and during MLSS settling tests can be significantly reduced with the use of an on-line MLSS settling meter.